

A Study on Packaging and Disinfection Effect of AlGaN Nanowire Deep UV LEDs

Wenqi Liang

Department of Electrical and Computer Engineering
McGill University, Montreal

April 2022

A thesis submitted to McGill University in partial fulfillment of the requirements of
the degree of **Master of Science**

© McGill, Wenqi Liang, 2022

To my parents, thank you!

Acknowledgements

First and foremost, I would like to thank my supervisor and mentor, Professor Songrui Zhao, for being understanding, patient, and supporting throughout my master's program. It is my honor to work under his supervision. His guidance, encouragement and professionalism have helped me overcome many challenges and difficulties, and they will continue to influence me throughout my life.

As a continuation of my undergraduate's design project, a special appreciation is given to my past teammates: Muxi Liu, Xijun Liu, and Lu Jin. Without their contributions to the design project, I would not have made this far on this research. I would like to thank all my colleagues in Zhao's lab: Heemal Parimoo, Qihua (David) Zhang, Mohammad Vafadar, Ricardo polo, Jiaying Lu and Xue Yin. It was my pleasure to work with so many nice and talented people. Special thanks to Heemal and David for helping me on the device measurements, and especially Heemal for giving me suggestions on the choices of much-needed coffee and accompanying me when we both need to work on multiple dues.

In addition, I am thankful to Dr. Chen Liang and Magan Solomon in the department of medicine for making themselves remotely available to me during collaborations and for any untimely questions I have. I am also grateful to the technical support provided by Electrolube and Botou Hi-tech, Dow Corning, McGill Nanotools and Microfab facility and the generous research funding from NSERC.

I am also grateful to my friends: Muxi Liu, Emily Zhang, and Weiyi Zhang for all the emotional support during my research and thesis writing. Lastly, I would like to express my deepest appreciation to my parents for always being supportive to me. This thesis would not come to a completion without their unspoken encouragement; therefore, this thesis is dedicated to them.

Abstract

Under pandemic circumstances, it is becoming increasingly important to improve the efficiency of disinfection systems. Among various disinfection systems, ultraviolet-C (UV-C, light emission wavelength less than 280 nm) germicidal irradiation is a well-known disinfectant, which is widely used for drinking and waste water treatment, air disinfection, and etc. In recent years, UV-C irradiation has been discovered to inactivate human coronavirus by destroying the outer protein coating. Traditionally, mercury vapor lamps are used to produce UV irradiation, with disadvantages including risks of toxic mercury release, long turn on/off time, large power consumption, and hardly practical for point-of-care treatment. Aluminum gallium nitride (AlGaN) UV-C light-emitting diodes (LEDs) offer a solution to overcome these issues. However, lack of efficient encapsulation material is one of major challenges in the development of UV-C LEDs based on AlGaN. In this thesis, we investigate the encapsulation and disinfection effects of AlGaN nanowire deep UV (DUV) LEDs emitting around 284 nm. Two different polymer materials: Polyurethane resin and silicone based dielectric material, are compared in this study. As for the disinfection effects, the effectiveness of AlGaN nanowire DUV LEDs in inactivating human coronavirus HCoV-229E is investigated. HCoV-229E is interested because it belongs to the same family Coronaviridae with the well-known SARs-CoV-2 and shares similar protein orders. An inactivation rate of 91.28% is obtained with a single $1 \times 1 \text{ mm}^2$ LED chip. Strategies to further improve the inactivation efficiency are further discussed in this thesis. This study shows that AlGaN nanowire DUV LEDs can be used as a promising UV source to construct an effective disinfection system against coronavirus.

Abrégé

Dans les situations pandémiques, il devient de plus en plus important d'améliorer l'efficacité des systèmes de désinfection. Parmi les différents systèmes de désinfection, l'irradiation germicide aux ultraviolets-C (UV-C, longueur d'onde d'émission lumineuse inférieure à 280 nm) est un désinfectant bien connu, largement utilisé pour le traitement de l'eau potable et des eaux usées, la désinfection de l'air, etc. Durant les dernières années, il a été découvert que l'irradiation UV-C inactive le coronavirus humain en détruisant le revêtement protéique externe. Traditionnellement, les lampes à vapeur de mercure sont utilisées pour produire une irradiation UV, mais avec des inconvénients tels que des risques de libération de mercure toxique, un long temps d'allumage/extinction, une grande consommation d'énergie et peu pratique pour les traitements au point de service. Les diodes électroluminescentes (LED) UV-C en nitrure de gallium et d'aluminium (AlGaN) offrent une solution pour surmonter ces problèmes. Cependant, le manque de matériau d'encapsulation efficace est l'un des défis majeurs dans le développement de LED UV-C à base d'AlGaN. Dans cette thèse, nous étudions les effets d'encapsulation et de désinfection des LED DUV à nanofil AlGaN émettant autour de 284 nm. Dans cette étude, deux matériaux polymères différents sont comparés : la résine polyuréthane et le matériau diélectrique à base de silicone. En ce qui concerne les effets de désinfection, l'efficacité des LED DUV à nanofil AlGaN dans l'inactivation du coronavirus humain HCoV-229E est étudiée. Le HCoV-229E est intéressant car il appartient à la même famille des Coronaviridae que le SARS-CoV-2 bien connu et partage des ordres protéiques similaires. Un taux d'inactivation de 91.28% est obtenu avec un seul puce LED de $1 \times 1 \text{ mm}^2$. Des stratégies pour améliorer encore l'efficacité de l'inactivation sont discutées plus en détail dans cette thèse. Cette étude montre que la LED DUV à nanofil AlGaN

peut être utilisée comme une source UV prometteuse pour construire un système de désinfection efficace contre le coronavirus.

Contribution of Authors

The dissertation work includes the contribution of the candidate and other individuals. The candidate and her supervisor, Prof. Songrui Zhao, defined the project and worked closely on the designs and experiment setups. Chapter 1 gives a summary of literature review. Chapter 2 presents a brief overview of AlGaIn nanowire LEDs. The devices used in this thesis study were fabricated by Prof. Songrui Zhao. The I-V characteristics of devices were measured with the help from Heemal Parimoo, and EL spectra were measured with help from Qihua (David) Zhang. The contribution of the candidate and others to the work presented in Chapter 3 – 5 is described as follows: In chapter 3, the mounting process is discussed and finalized in the design project group: Muxi Liu, Lu Jin, Xijun Liu and the candidate. The candidate and Muxi Liu contributed to finalizing wire bonding procedure and performing wire bonding experiments. In chapter 4, Lu Jin and the candidate contributed to the shape design. UR5638 epoxy resin was researched by Lu Jin, and EI-1184 was researched by the candidate. In chapter 5, UR5638 material test was performed by Lu Jin. EI-1184 material test and encapsulation of AlGaIn nanowire DUV LED die on TO-header were performed by Lu Jin and the candidate. In Chapter 6, the disinfection experiment was designed and led by Prof. Songrui Zhao, Dr. Chen Liang, Magan Solomon, and the candidate. The experiments were performed with help from Magan Solomon. Candidate contributed significantly to sample preparation, designing experiment setup, virus placement, experimental condition estimation, and data analysis.

Table of Contents

Acknowledgements.....	3
Abstract	4
Abrégé.....	5
Contribution of Authors	7
Table of Contents	8
Figure List	11
Table List.....	13
Abbreviation List	14
CHAPTER 1: Introduction.....	15
1.1 Background on Coronavirus and UV Inactivation.....	15
1.2 The Need of UV LED Technology and Current Status.....	19
1.3 Necessities and Challenges in Packaging	21
1.4 Thesis Objective	23
CHAPTER 2: AlGa_N Nanowire DUV LEDs	24
2.1 The Need of AlGa _N Alloys for DUV LEDs.....	24
2.2 AlGa _N Nanowire DUV LEDs	26
2.2.1 Characteristics of AlGa _N Nanowire DUV LEDs Used in This Thesis Study	27
CHAPTER 3: Mounting LED Die to TO-Header.....	30
3.1 Overview.....	30
3.2 Key Components	31
3.2.1 TO-header	31
3.2.2 Silver Epoxy.....	31

3.2.3 Hot Plate.....	32
3.2.4 Breadboard.....	32
3.3 Key Steps	32
3.3.1 Chip Dicing	32
3.3.2 Wire Bonding	33
3.3.3 Probing.....	33
3.4 Tools and Equipment for the Mounting Process.....	34
CHAPTER 4: Encapsulation Design Considerations	36
4.1 Background on the Light Extraction of LEDs	36
4.2 Shape Consideration.....	37
4.3 Material Consideration	39
CHAPTER 5: Encapsulation Results	42
5.1 Curing Process and Transmittance	42
5.1.1 UR5638	42
5.1.2 EI-1184.....	43
5.1.3 Tools and Materials for Curing and Transmittance Measurement	45
5.2 Encapsulation of AlGa _N Nanowire DUV LED Die on TO-header	45
CHAPTER 6: Disinfection Experiments	47
6.1 Disinfection Experiments on Bare AlGa _N Nanowire DUV LEDs	47
6.1.1 Setup	47
6.1.2 Virus Placement.....	48
6.1.3 Experimental Condition Estimation	49
6.1.4 Experimental Procedure.....	51

6.1.5 Results	51
a) Control Experiments	51
b) Disinfection Experiments	52
6.1.6 Tools and Materials	55
6.2 Disinfection Experiments on AlGa _N Nanowire DUV LEDs Covered with EI-1184	55
CHAPTER 7: Conclusions and Future Work.....	58
References.....	60

Figure List

Figure 1: Characteristics of coronaviruses. A) Coronaviruses family tree. B) Genome organizations, C) overall base composition, and D) adjacent base arrangement of SARS-CoV-2, HCoV-OC43, and HCoV-229E [17].	17
Figure 2: Effectiveness of UV irradiation to inactivate SARs-CoV [28].	18
Figure 3: Effectiveness of UV-C LEDs to inactive HCoV-229E at different wavelength [17].	19
Figure 4: A visible LED encapsulated by Hysol® OS4000 epoxy [53].	21
Figure 5: Different packaging designs for DUV LEDs [43].	23
Figure 6: Energy bandgap versus its bond length of various materials [61].	25
Figure 7: EQE for near and DUV LEDs based on semiconductor AlGaIn [37].	26
Figure 8: I-V characteristics of AlGaIn nanowire DUV LEDs.	27
Figure 9: EL spectra of an AlGaIn nanowire DUV LEDs.	28
Figure 10: LOP of AlGaIn nanowire DUV LEDs at 284 nm.	29
Figure 11: Schematic of a mounted LED die.	30
Figure 12: Top view of TO-39 header. The dimensions are described in the main text.	31
Figure 13: A photo of post-wire bonding probing. It is seen that the device lights up when the probing needle touches the thin bonding wire.	34
Figure 14: Schematic of light propagation in a planar LED chip.	37
Figure 15: Schematic of light propagation with a dome shape encapsulation.	38
Figure 16: Schematic of a dome shape encapsulation.	38
Figure 17: Transmittance of siloxane-modified epoxy resins [80].	39
Figure 18: Transmittance of EI-1184 with a thickness of 3.2 mm [87].	41
Figure 19: Cured UR5638 resins.	43

Figure 20: Cured EI-1184 resins.....	44
Figure 21: Transmittance of bare EI-1184.	44
Figure 22: Image of encapsulated AlGaIn nanowire DUV LED die.	45
Figure 23: Schematic of the circuit setup.	48
Figure 24: Schematic of the setup for disinfection experiments with non-encapsulated AlGaIn nanowire DUV LED wafers.....	49
Figure 25: Illustration of the relation between volume and surface area for water. (a) Table of spot surface area, volume, diameter, volume to surface area ratio from experiment and geometrically derived. (b) Marked sketch of cross section. (c) Image of 1.5 μ L water on glass surface [93].....	50
Figure 26: RLU as a function of time without UV-C irradiation from AlGaIn nanowire DUV LEDs.....	52
Figure 27: (a) RLU and (b) infectivity as a function of time with 5 mA applied current.	53
Figure 28: (a) RLU and (b) infectivity with respect to time with 10 mA applied current.	54
Figure 29: Schematic of disinfection test setup with encapsulant.	56
Figure 30: Image of AlGaIn nanowire DUV LED wafer covered by EI-1184 in a near flat shape.	57

Table List

Table 1: List of tools and equipment for the mounting process	35
Table 2: List of materials and tools for curing and transmittance measurement	45
Table 3: List of materials and tools for encapsulation	46
Table 4: List of materials and tools for disinfection experiments	55

Abbreviation List

UV	Ultraviolet
DUV	Deep Ultraviolet
TCID ₅₀	50% tissue culture infectious dose assay
CPE	Induce cytopathic effects
LED	Light Emitting Diode
PFU	Plaque Forming Units
RI	Refractive index
Si-O	Silicon Oxide
SARS-CoV-2	Severe Acute Respiratory Syndrome Coronavirus 2
NaClO	Sodium Hypochlorite
HCoV	Human Coronavirus
AlGaN	Aluminum Gallium Nitride
EL	Electroluminescence
EQE	External Quantum Efficiency
IQE	Internal Quantum Efficiency
LEE	Light Extraction Efficiency
IE	Injection Efficiency
RRE	Radiative Recombination Efficiency
LOP	Light output power
PDMS	Polydimethylsiloxane
RLU	Relative luminescence unit
TIR	Total internal reflection

CHAPTER 1

Introduction

Ultraviolet (UV) light has a shorter wavelength than visible light and ranges from 200 nm to 400 nm. Its radiation wavelength is classified into UV-A (320 – 400 nm), UV-B (280 – 320 nm), and UV-C (200 – 280 nm). As an element of sunlight, its effects on skin, plants, and microbes have been studied, and it can be both beneficial and harmful to human [1-6]. Thus, photonic devices which emit UV light are invented to carry forward the beneficial effects. Among the wide range of UV spectrum, UV-C photonic devices play an important role in various fields such as water purification, bioagent sensing, and food or medical sterilization [7-11]. In the presence of current pandemic outbreak, UV-C light emitting devices become critically important due to their high inactivation rate against coronavirus, which can potentially provide a new avenue for surface disinfection.

1.1 Background on Coronavirus and UV Inactivation

A contagious coronavirus 2019 disease, which is caused by Severe Acute Respiratory Syndrome Coronavirus 2 (SARS-CoV-2), has been spread worldwide, and the World Health Organization (WHO) declared this outbreak as pandemic in March 2020. More than 517 million infections and 6 million deaths have been reported at the time of writing this thesis [12]. In addition to this, there are many unconfirmed and unreported cases, given the high incidence of asymptomatic cases escaping the capture by traditional diagnostic and detection methods.

In general, for coronaviruses, it can be classified into four genera: the Alpha (α -), Beta (β -), Gamma (γ -) and Deltacoronavirus (δ -coronavirus). Among the different genera, α -coronaviruses

and β -coronaviruses are found to cause various human respiratory infections, and it is noted that SARS-CoV-2 variants (e.g., δ -variant) belong to the β -coronavirus group, whereas δ -coronavirus is another group of coronavirus species, which only resides in birds and occasionally in non-human mammals [13].

Beside SARS-CoV-2, there were two deadly coronavirus outbreaks in the past caused by MERS-CoV and SARS-CoV, and both belong to β -coronaviruses [14-16]. Human Coronavirus OC43 (HCoV-OC43) and HCoV-HKU1 are two other known infectious species in β -coronaviruses. As for α -coronaviruses, HCoV-229E and HCoV-NL63 are known to be infectious to human. Human coronaviruses including HCoV-229E, HCoV-NL63, HCoV-OC43 and HCoV-HKU1 are spread endemically at different times of the year and cause 15-30% respiratory infections [14].

Fig. 1A demonstrates different genera and branches of coronaviruses. Genomic organizations are shown in Fig. 1B. Nonstructural proteins are shown to be identical for SARS-CoV-2 and HCoV-229E, and structural proteins have similar order in the same form of spike, envelop, membrane and nucleocapsid proteins. It has also been found by Ong et al. that the overall base composition and adjacent base arrangements are very similar, as shown in Fig. 1C and Fig. 1D [17]. Therefore, performing experiments on HCoV-229E gives representative results of inactivation efficiency of the coronavirus family, which is the focus of this thesis work.

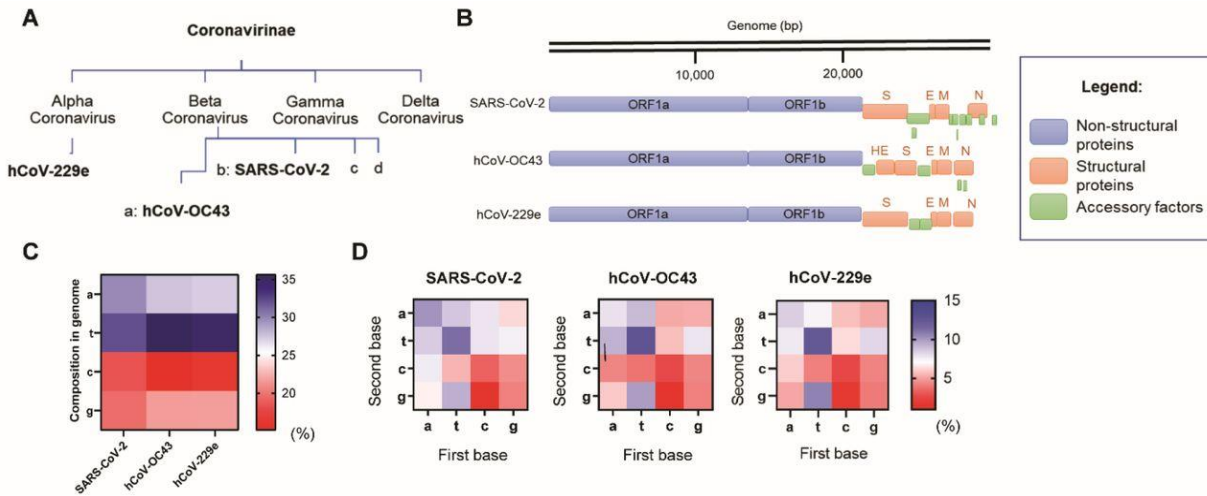


Figure 1: Characteristics of coronaviruses. A) Coronaviruses family tree. B) Genome organizations, C) overall base composition, and D) adjacent base arrangement of SARS-CoV-2, HCoV-OC43, and HCoV-229E [17].

To combat SARS-CoV-2, preventions including vaccination, masking, hand sanitizing have been blended into people’s daily life in combating virus spread within communities [18-20]. Disinfection products including 0.05% sodium hypochlorite (NaClO) and ethanol with 70% concentration have been used to eliminate viruses on surfaces and objects [21, 22]. Among all the new emerging disinfection methods, UV irradiation as a chemical-free technology attracts researchers’ attention and has been rapidly growing in inactivating viruses, bacteria and other microbes [17, 23, 24].

UV light inactivates microbial cells by damaging the intracellular components of microbes including RNA and DNA. With different wavelengths, UV irradiation affects viruses differently. RNA and DNA are sensitive to UV-C irradiation, and the ability of viruses to replicate can be heavily influenced by absorbing UV-C photons so that they can no longer infect human cells. UV-B is found to be 20 to 100 fold less effective compared with UV-C irradiation. Although UV-A is weakly absorbed by RNA and DNA, additional genetic damage can be caused by UV-A irradiation such as causing bases oxidation and strand breaks through the formation of reactive oxygen species

[23, 25-27]. UV-C is the current focus on inactivating coronavirus because its ability is shown to be more effective in numerous studies.

Miriam et al. performed a set of experiments by using 254 nm UV-C radiation source and 365 nm UV-A light source on SARS-CoV to examine the change in infectious dose [28, 29]. 50% tissue culture infectious dose assay (TCID₅₀) was used to quantify the amount of infectious virus particles. By incubating serial dilutions of virus samples, the amount of virus dilution that required to induce cytopathic effects (CPE) in 50% infected samples is measured. The results are shown in Fig. 2. There are no significant changes in the UV-A irradiation control group, whereas the UV-C irradiation shows significant inactivation effect on SARS-CoV. Same results have also been demonstrated in the study by Chiappa et al., wherein UV-C light shows the most potent effect in inactivating micro-organisms including viruses, bacteria, and etc. [30].

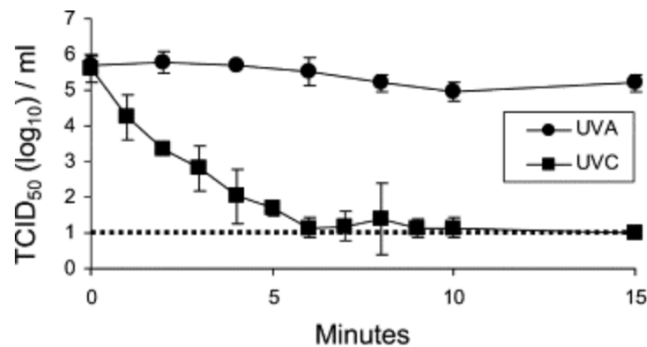


Figure 2: Effectiveness of UV irradiation to inactivate SARS-CoV [28].

The behavior of inactivating HCoV-229E virus using light emitting diodes (LEDs) emitting at different UV-C wavelengths (222 nm, 254 nm, and 277 nm) has been also studied. The infectivity is determined by comparing the Plaque Forming Units (PFU), which is another method of quantifying infectious. The results are shown in Fig. 3. Although the mechanism of the relation between UV-C wavelengths and the effectiveness of inactivation is still being investigated, 277 nm is found to show the best results on HCoV-229E among 222, 254, and 277 nm. The experiment

setup used a 5×5 array of UV-C LEDs at a beam angle of 120 degree and a working distance of 12 cm. The UV intensity of all experiments remained consistent at $73 \mu\text{W}/\text{cm}^2$ [17].

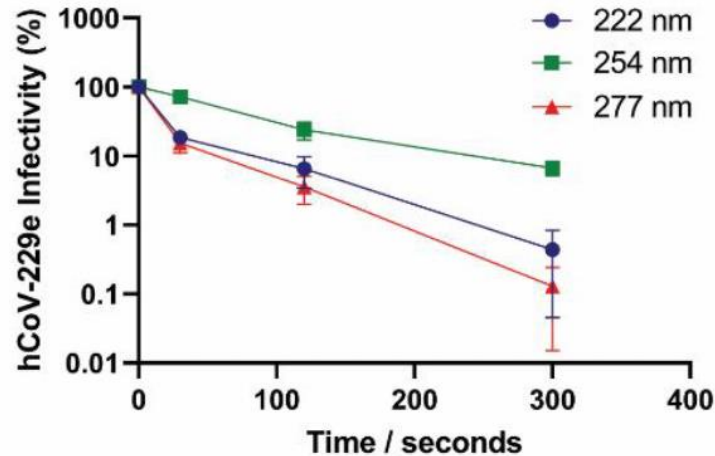


Figure 3: Effectiveness of UV-C LEDs to inactive HCoV-229E at different wavelength [17].

Besides these studies, others have shown that SARS-CoV-2 and other coronavirus species exhibit the highest sensitivity among UV-C wavelengths of 265 nm and 267 nm than other wavelengths such as 280 nm, 286 nm, and 297 nm, with the fastest disinfection responses and the lowest UV doses applied [31, 32].

There have been numerous studies that demonstrate the inactivation efficiency of deep ultraviolet (DUV) irradiation; however, there are still many research aspects that are still under investigation, such as wavelength versus inactivation efficiency, LED versus germicidal lamps, and so on. In this thesis, the inactivation effect of aluminum gallium nitride (AlGaIn) nanowire 284 nm LED devices is studied.

1.2 The Need of UV LED Technology and Current Status

In conventional UV technologies, UV light is generated with an electric arc through vaporized mercury under pressure. Quartz glass materials are highly used in the germicidal

mercury lamps and pose a risk of toxic mercury release [33]. High power consumption and long warm up/cool down time are two other challenges manifested in practical applications. Alternatively, UV LED technology as a point light source is developed rapidly with instant turn-on/off time, low power consumption, and large design flexibility especially in small scale applications. Given these advantages of the UV LED technology, researchers and industry practitioners are encouraged to consider it as an alternative UV source [3, 29, 34, 35].

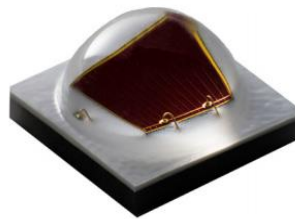
From the view of the commercial LED market, UV-A LEDs (350 – 390 nm) offer significant advantages over mercury or fluorescent due to the increased efficiency, lower cost of ownership and system miniaturization. They are highly used in 3D printing, UV curing, lithography, sensing, security, and so on. Due to the cost efficiency and the mature level, UV-A LEDs have been dominating the current market comparing to UV LEDs in other wavelengths [7, 36, 37]. The “lower” UV-A and “upper” UV-B range (300 – 350 nm) is the most recently-introduced range to the market. Devices in this range offer the potential for a variety of applications including UV curing, biomedical and DNA analysis, and 3D printing, but the overall cost is still relatively high [36, 38].

The “lower” UV-B and “upper” UV-C range (approximately 250 – 300 nm) is a range that is still under investigation and gradually enters the stage of commercial mass production. Due to the effectiveness in air and water disinfections, there is an increasing demand for UV-C LEDs since 2019, and the high demand drives the LED market growth in “lower” UV-B and “upper” UV-C range. Further due to the adverse impact of SARS-CoV-2, LED segment in “lower” UV-B and “upper” UV-C range is expected to grow at a fast rate and dominate the market in the near future [7, 36, 38, 39].

1.3 Necessities and Challenges in Packaging

LED packaging involves many stages in the manufacturing process, such as dicing, wire bonding, encapsulation, and lens mounting. The reliability and performance of an LED depend on the design of LED packaging. Researchers have been working to improve every step of LED packaging [40-43]. To extract maximum light out of LED chips, encapsulation and lens play significant roles. Moreover, because bare LED devices are vulnerable to many factors in the environment, encapsulation is necessary. Factors such as moisture and dust in the air, vibration, mechanical and thermal shocks, among others, in the real working condition can all affect the performance of LED devices and accelerate the device degradation [44-51]. Therefore, encapsulation is important in improving the device robustness and stability. For example, in a water-rich environment, encapsulation can protect the electronics from the corrosion of metals and enhance the overall lifetime of the device.

Current commercial LEDs that are widely used in industries and daily lives have well-developed packaging design, including the choice of material and implementation procedure. Inexpensive and easy-to-process organic encapsulants are used for visible LEDs. For example, for LEDs operating between 450 nm and 470 nm, Hysol® OS4000 epoxy is a commonly used encapsulation material by CREE LED. An encapsulated visible LED is shown in Fig. 4 [52, 53].



XP-G3 Photo Red

Figure 4: A visible LED encapsulated by Hysol® OS4000 epoxy [53].

However, for LEDs operating in DUV spectral range, e.g., light emission wavelength below 300 nm, efficient encapsulation technology remains challenging and is still under investigation. Currently-in-use organic polymeric encapsulation materials for visible LEDs are not applicable to DUV LEDs due to challenges such as UV absorption and UV yellowing, which cause reduction of transparency, decreasing of light extraction efficiency (LEE), and loss of reliability [43, 54]. The UV radiation induced changes in polymers are mainly from the carbon-carbon double bonds, which absorb UV light and shift the surface color [55, 56]. As such, polymers with fewer carbon to carbon double bonds are more UV radiation resistant [56].

Silicone as an “inorganic synthetic polymer [57]” has been studied for DUV LED encapsulation, due to its good thermal and UV resistance [54, 58]. Its inorganic silicon-oxygen (Si-O) bonds protect the polymer bonds from damaging under UV exposure [58]. Moreover, researchers have found that certain organic polymers can be UV radiation resistant, such as polyethylene and polyurethane.

In parallel, packaging without using any encapsulation materials has been investigated as well, in order to avoid issues associated with encapsulation materials under DUV irradiation. For example, as shown in Fig. 5(a), a glass lens is used as a transparent window on top of a TO-header, and metal can creates a confined space [43]. In Fig. 5(b), another design with a three-dimensional substrate structure has also been used, with a quartz plate bonded on the top [43]. In both designs, conventional encapsulation materials are no longer needed because the sealed space offers the protection to the LED chip against moist and dust in the environment, partially fulfilling the encapsulation purpose. However, these designs are often associated with a relatively high manufacturing cost due to the complicated fabrication process.

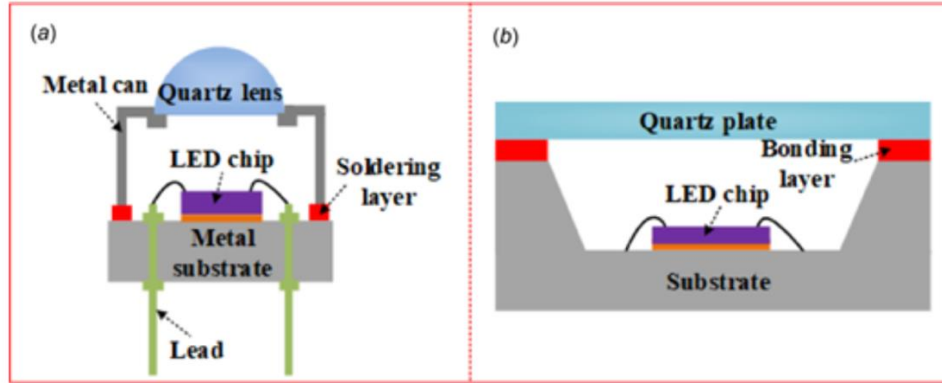


Figure 5: Different packaging designs for DUV LEDs [43].

In this study, conventional packaging method is investigated. Polyurethane resin and silicone-based materials are compared to study whether the UV resistant organic polymer or the inorganic synthetic polymer is better for DUV LED encapsulation.

1.4 Thesis Objective

The objective of this thesis is to investigate the encapsulation and disinfection effects of AlGaIn nanowire DUV LEDs emitting at around 284 nm. There are two major tasks in this thesis: LED device packaging including the study on the encapsulation materials, and disinfection experiments. Chapter 2 describes the basic properties of AlGaIn nanowire DUV LEDs used in this thesis study. Packaging of such nanowire DUV LEDs, which includes mounting LED die to TO-header and encapsulation, is discussed from Chapter 3 to Chapter 5, with Chapter 3 describing the mounting of the LED die to the TO-header, Chapter 4 describing the encapsulation design considerations, and Chapter 5 describing the results of encapsulation including the transmittance of the polymers investigated in this thesis study. This is followed by disinfection experiments in Chapter 6, wherein the effectiveness of AlGaIn nanowire DUV LEDs as disinfectant is tested. Conclusions and future work are presented in Chapter 7.

CHAPTER 2

AlGaN Nanowire DUV LEDs

In this chapter, the materials aspect of this thesis, i.e., the materials used for the fabrication of DUV LEDs in this thesis study, is discussed. In Section 2.1, the need of AlGaN alloys for DUV LEDs, together with the challenges, is discussed. In Section 2.2, properties of AlGaN nanowire DUV LEDs used in this thesis are discussed, including both the electrical and optical properties.

2.1 The Need of AlGaN Alloys for DUV LEDs

Among various semiconductor materials, AlGaN draws special attention because of its tunable bandgap energies from 3.4 eV to 6.2 eV by altering the composition of Al and Ga. The wavelength corresponding to its bandgap is approximately 207 to 364 nm by using Eq. 1, whereas E is the bandgap energy, λ is the wavelength [59, 60].

$$E = hv = h \frac{c}{\lambda} \quad (1)$$

In Fig. 6, various materials and their corresponding bandgap energies are shown. It is seen that, for the DUV spectral range between 200 to 300 nm, AlGaN alloy system is the most promising candidate.

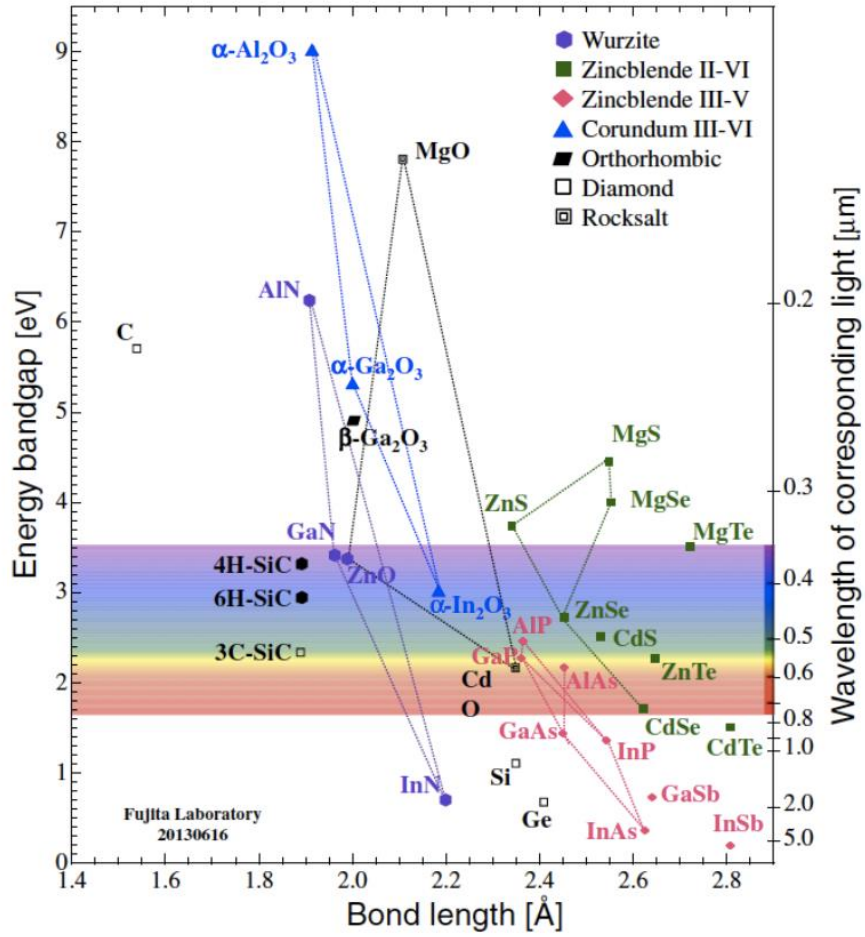


Figure 6: Energy bandgap versus its bond length of various materials [61].

However, the overall efficiency of AlGaIn thin film DUV LEDs remains relatively low. There are several challenges such as difficulty in crystal growth, poor p-type doping, and low LEE. Currently, the best external quantum efficiency (EQE) demonstrated so far for devices in the DUV range is around 20% [37]. EQE is the commonly used parameter to characterize the performance of LED devices, and the EQE of DUV LEDs is significantly lower compared to that of devices in the near UV wavelength range, as shown in Fig. 7. The EQE, η_{EQE} , is directly proportional to the internal quantum efficiency (IQE), η_{IQE} , and LEE, η_{ext} , and can be calculated by Eq. 2:

$$\eta_{EQE} = \eta_{IQE} \times \eta_{ext} = \eta_{inj} \times \eta_{rad} \times \eta_{ext} \quad (2)$$

Thus, IQE and LEE play significant roles in the final device performance [37, 40, 62]. As for IQE, it is a product of injection efficiency (IE), η_{inj} , and radiative recombination efficiency (RRE), η_{rad} , also shown in Eq. 2.

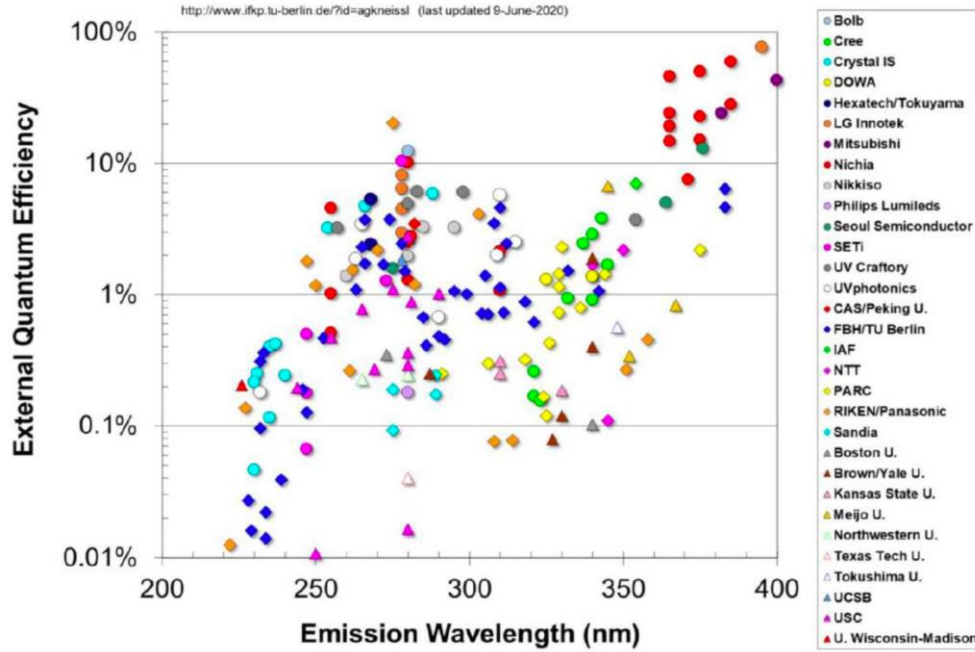


Figure 7: EQE for near and DUV LEDs based on semiconductor AlGaN [37].

2.2 AlGaN Nanowire DUV LEDs

In this context, nanowires may become an emerging solution for various challenges facing AlGaN thin film DUV LEDs. For example, the use of nanowires allows stress (from lattice mismatch between AlGaN and substrates as well as GaN and AlN) to relax efficiently to lateral surfaces due to the large surface to bulk volume ratio of the nanowire geometry, so that better material quality can be obtained, which can thus potentially improve RRE [63-65]. In addition, the doping concentration in nanowire structures is also higher than that in planar counterparts [65-68]. Thus, the conductivity increases, which is favourable for electrical injection.

2.2.1 Characteristics of AlGaN Nanowire DUV LEDs Used in This Thesis Study

Fabrication of such AlGaN nanowire DUV LEDs can be found in [67]. The typical I-V characteristics of such LEDs are shown in Fig. 8. In this experiment, square-shaped devices with an area of $1 \times 1 \text{ mm}^2$ were measured. According to the bandgap energy of AlGaN, the turn-on voltage should be less than 6 V. A higher turn-on voltage of the present devices reflects non-optimized electrical doping and electrical contact, which are currently under optimization.

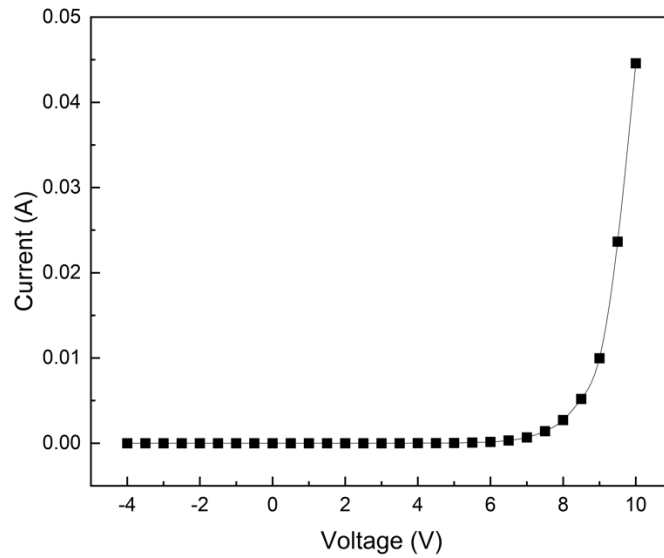


Figure 8: I-V characteristics of AlGaN nanowire DUV LEDs.

Fig. 9 shows the electroluminescence (EL) spectra of a typical AlGaN nanowire DUV LED device used in this thesis under injection currents varying from 1 mA to 16 mA. The EL peak wavelength is approximately at 284 nm. There is a slightly blue shift of the EL peak as the current increases, due to the screening of quantum-confined Stark effect as the injection current increases. In such experiments, the EL emission was collected by an optical fibre from the device top surface.

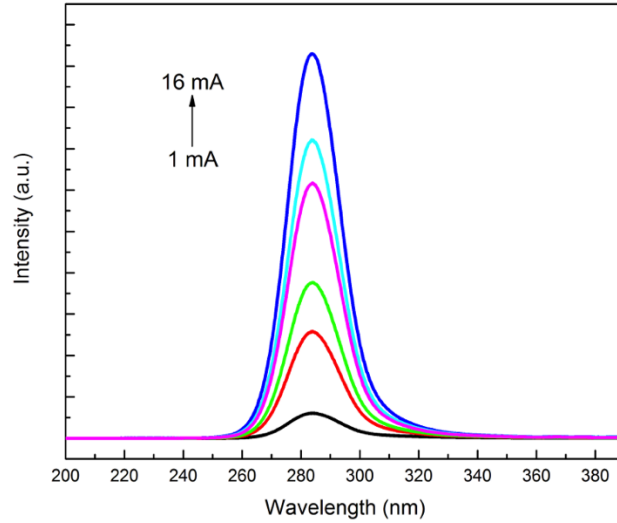


Figure 9: EL spectra of an AlGaIn nanowire DUV LEDs.

The light output power (LOP) was further measured. The LOP is defined as the energy of light generated per unit time and can also be specified as Watt or Joules per second. It is a measurement of the brightness of an LED device [69, 70]. The LOP is proportional to EQE. In this thesis study, the LOP was measured by a Si-based photodetector, which was placed a few mm above the device top surface (bare surface). Fig. 10 shows the LOP of AlGaIn nanowire DUV LEDs used in this thesis study with different sizes under various injection currents. It is seen that the LOP increases as the injection current increases. The device size dependent LOP could be due to the efficiency droop at higher current densities [67].

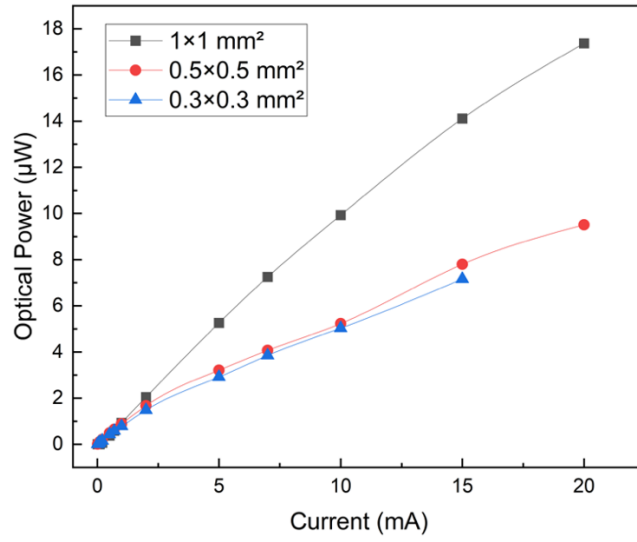


Figure 10: LOP of AlGaIn nanowire DUV LEDs at 284 nm.

CHAPTER 3

Mounting LED Die to TO-Header

As mentioned in the thesis organization, the packaging of AlGaIn nanowire DUV LEDs is separated in two parts: mounting LED die to TO-header and encapsulation. This chapter discusses the mounting process. In Section 3.1, an overview of the mounting process is described, followed by the discussions of key components used in Section 3.2 and key steps involved in Section 3.3, respectively. Tools and equipment used in the mounting process are listed in the end in Section 3.4.

3.1 Overview

Fig. 11 shows a schematic of an LED die on a TO-header. The metal contact on the LED die is first bonded with a thin bonding wire by silver epoxy. The backside of the LED die is then electrically connected to the TO-header using silver epoxy. Silver epoxy is also used to connect the other end of the bonding wire with the isolated pin of the TO-header. In this way, LED die is mounted to a TO-header. In the following sections, we describe the key components and steps in this mounting process.

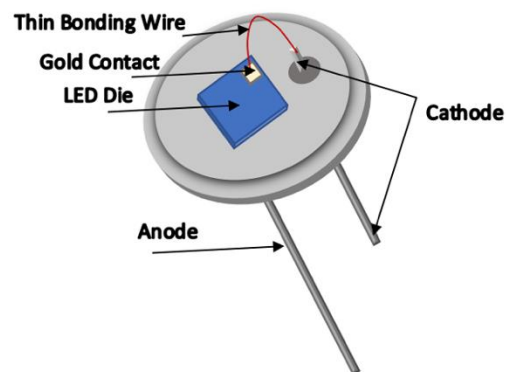


Figure 11: Schematic of a mounted LED die.

3.2 Key Components

3.2.1 TO-header

TO-39 header has 4 pins, including one ground and three isolated pins, and the diameter is 9 mm as illustrated in Fig. 12. The maximum die dimension can be held on the header plate is 3 mm × 3 mm. In this thesis, by polishing the surface of TO-39, two unused pins were removed to allow the header to hold LED die that has larger dimensions. Maximizing the plate size of TO-39 could simplify the encapsulation process. Square shaped die was targeted in this process, with an intended width of around 5 mm. With this width, LED die can fit onto the TO-39 header without surpassing the edge of the header plate.

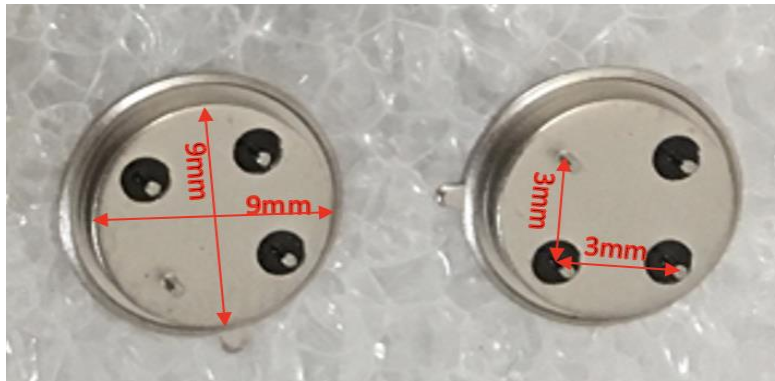


Figure 12: Top view of TO-39 header. The dimensions are described in the main text.

3.2.2 Silver Epoxy

In this study, EPO-TEK H20E silver epoxy was used for wire bonding due to the advantages of high reliability and stability. The epoxy includes two separate parts and can be formed by mixing the two parts by a weight ratio of 1:1. The curing temperature of the epoxy is 150 °C for 5 minutes. In comparison, liquid-based colloidal silver paste has an easier curing

process and is commonly used when the robustness of the connection is not required. Another advantage of the liquid-based silver paste is its easy removal.

3.2.3 Hot Plate

In this study, hot plate was mainly used to cure the silver epoxy to stabilize the electrical connection at both the metal contact side of the device and the pin side of the header. Each sample was cured at 150 °C for 5 minutes.

3.2.4 Breadboard

In this study, the breadboard was used in the electrical test after mounting the LED die to the TO-header. By connecting the anode with the positive terminal and the cathode with the negative terminal on the breadboard, current can be supplied to the mounted LED chip. Breadboard was also used in the electrical test after encapsulation, which will be discussed in Chapter 5.

3.3 Key Steps

3.3.1 Chip Dicing

To fit the dimensions of TO-header, the LED wafer needs to be cut into small pieces (LED die). Dicing saw is commonly used to cut semiconductor wafer into intended sizes. It provides accurate control on the size of LED die. In general, there is a minimum achievable size for a dicing saw. During the dicing process, de-ionized water (DI water) is commonly used as a coolant and lubricant for the blade and the material. It is also used to flush away swarf particles [71, 72]. The water flushing process could wash away small dies, limiting the minimum achievable die size. Moreover, if the intended die size is too small, there is a risk of breaking the blade.

The dicing saw in McGill Nanotools and Microfab facility cannot control sizes less than 1 cm precisely. As an alternative option, the LED wafers were manually separated into small pieces by using natural cleaving with a diamond pencil under microscope. To obtain the best dicing results, $1 \times 1 \text{ mm}^2$ LED devices with the highest LOP were centered in the intended die so that the risk of destroying such LED devices by the diamond pencil was minimized.

3.3.2 Wire Bonding

Conventional wire bonding process uses a wire-bonder. However, the top surface metal contact of AlGaIn nanowire DUV LEDs used in this thesis study is a thin metal layer, and the thin metal layer peeled off during the bonding process under the available power and pressure conditions. Therefore, as an alternative method, silver epoxy was used to manually bond the wire between the thin metal contact of the AlGaIn nanowire DUV LEDs and the isolated pin of the TO-header.

3.3.3 Probing

Probing is a commonly used method to measure the electrical properties of electrically injected devices. In the probing process, an electrically conductive probe touches the metal contact of the device, through which the electric current is injected into the device. In this thesis, probing was used in different stages of LED packaging.

Before chip dicing was performed, probing was used to identify the areas of the wafer that could be further processed into LED dies. Ideally, large size, high LOP, and non-leaky devices are given the priority.

After the chip dicing process, it is also important to re-examine the devices that are intended to be used in the wire bonding process by probing, and this is to ensure that the devices intended

to be wire bonded are working devices. Experimentally, for each die, the locations of targeted devices were marked so that they could be distinguished for the next step processing.

Post-wire bonding probing was also implemented after connecting the thin metal pad of the device with the thin bonding wire using silver epoxy. The purpose is to check if the wire bonding is successful or not. For LED die with a good wire bonding, it was further mounted to the TO-header. Fig. 13 shows a well bonded device from a large area wafer, used for the post-wire bonding probing illustration purpose. It is seen that the device lights up when the probing needle touches the bonded thin wire.



Figure 13: A photo of post-wire bonding probing. It is seen that the device lights up when the probing needle touches the thin bonding wire.

3.4 Tools and Equipment for the Mounting Process

The table below lists the tools and equipment in the mounting process. The mounted LED die will be shown in Chapter 5 together with the encapsulation.

Table 1: List of tools and equipment for the mounting process

Basic Circuit Elements	
Breadboard	830 Tie points with size 2.2" × 7"
TO-39 header plate	9 mm; 4 pins; multiple pieces
Dicing Tools	
Tweezers	2 pairs
Diamond pencil	1
Gloves for protection	multiple
Wire-Bonding Tools	
EPO-TEK- H20E silver epoxy	1 oz part A, 1 oz Part B
Thin bonding wires	5 m
Hot plate	1 unit
LED Device Probe Tools	
AlGaIn nanowire DUV LEDs	multiple
Keithley source meter	1 unit
Optical microscope	1 unit
Needle pins	2
Tweezers	2 pairs

CHAPTER 4

Encapsulation Design Considerations

LED encapsulation includes adding liquid epoxy onto the surface of the LED device and baking until the epoxy is cured. This chapter introduces the encapsulation design considerations in terms of shape and materials used for encapsulation. In Section 4.1, background knowledge on the light extraction of LEDs is first presented. Shape consideration is then discussed in Section 4.2, followed by the consideration on the choices of encapsulation materials in Section 4.3.

4.1 Background on the Light Extraction of LEDs

According to the Snell's law, the refracted angle (θ_2) in air is determined by the incident angle of the light ray in semiconductor (θ_1) as shown in Eq. 3:

$$n_s \sin \theta_1 = n_a \sin \theta_2 \quad (3)$$

where n_s and n_a are the refractive indices (RIs) of the semiconductor and the air, respectively. The critical angle is an important parameter, and it is the greatest angle that a light ray can travel to the second medium (air) without being reflected in the first medium (semiconductor). For angles greater than the critical angle, total internal reflection (TIR) occurs. For angles less than the critical angle, the light ray can be refracted out. As such, the critical angle defines a light escape cone, which further relates to the amount of light that can be extracted and LEE. Fig. 14 illustrates the light escape cone and the light propagations for a planar LED chip without packaging.

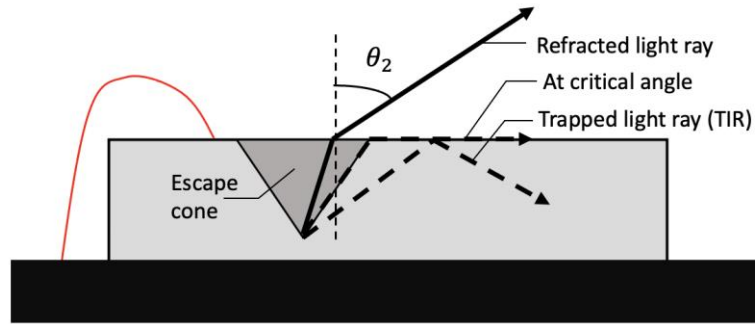


Figure 14: Schematic of light propagation in a planar LED chip.

4.2 Shape Consideration

By applying an additional encapsulation layer, the escape cone of LEDs could increase according to the Snell's law as illustrated in Fig. 15. This is because typically encapsulation materials have higher RIs than that of air, therefore, as the light travels to the semiconductor and encapsulation interface, the refracted angle in the encapsulation material is smaller than the refracted angle in air ($\theta_2' < \theta_2$), so that more light can be refracted out of the semiconductor into the encapsulation material without being reflected. In this way, the light extraction of LEDs can be improved with encapsulation.

Fig. 15 also illustrates how the light propagates with a dome shape encapsulation. Proper dome shape allows the light incident angle to be perpendicular to the encapsulation surface. As the incident angle approaching 0° , no refraction occurs; as such, a straight light propagation line can be obtained. In this way, more light can be refracted out of the encapsulation material. Specifically, Fresnel reflection loss, which caused by TIR, is reduced at the encapsulation and air interface [73].

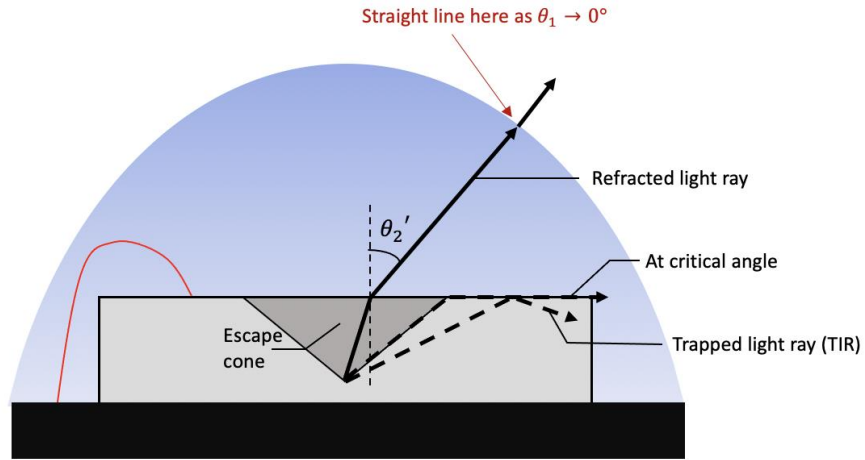


Figure 15: Schematic of light propagation with a dome shape encapsulation.

Schematically shown in Fig. 16, a dome shape can be defined by the height h and the radius r . To analyze the geometry of different dome shapes, Consonni et al. (2011) have performed Monte Carlo simulations to optimize the light extraction [74]. The study provides a guidance of different dome shapes. Height to radius ratios of 0.3, 0.7, 1, 1.3, and 1.7 have been simulated and analyzed. Overall, a height to radius ratio of 0.7 has shown the best performance. However, practically, this finding might not be applicable to this thesis due to the difference in the encapsulation material [74-76]. Therefore, dome shapes with different height to radius ratios are prepared in this thesis study, and the results will be discussed in Chapter 5.

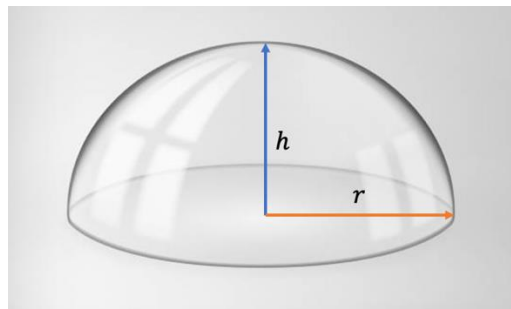


Figure 16: Schematic of a dome shape encapsulation.

4.3 Material Consideration

The first consideration from the materials aspect is that the materials used for encapsulation have RIs closer to that of the semiconductor [74, 77]. AlGaIn has a high RI of 2.557 at 310 nm [78]; consequently, in order to better extract light from AlGaIn UV LEDs around this wavelength, a material with RI close to 2.5 is preferred.

Another consideration is the light transmittance of the materials at the intended wavelength. Unfortunately, most of the resins for encapsulation are limited to wavelengths longer than 360 nm. The transmittance drops drastically below 360 nm, and thus the transmittance in the DUV spectral range is barely studied [79-81]. For example, as shown in Fig. 17, siloxane-modified epoxy resins exhibit high transmittance in near UV spectral range. However, there is a clear drop below 400 nm, and there is no measurement of transmittance in DUV spectral range [80]. In this thesis study, extensive material search has been carried out based on the LED operating wavelength, and two products with high RIs and high transmittance at 380 nm were found: UR5638 polyurethane resin and DOWSIL EI-1184 gel.

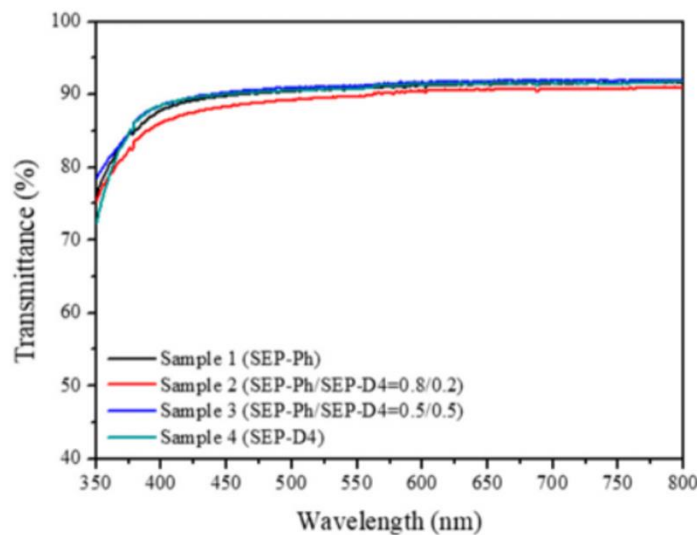


Figure 17: Transmittance of siloxane-modified epoxy resins [80].

UR5638 is a polyurethane-based resin with a high RI of 1.481 and a low water absorbance of less than 1% at the room temperature. In comparison with the thermal conductivity of air (“0.025 W/m K [82]”), UR5638 exhibits a higher thermal conductivity of 0.30 W/m K [83]. It also has remarkable properties such as low exotherm, superior UV stability, and excellent transmission for UV light. As a polyurethane-based resin, UR5638 is also able to provide a clear, transparent finish. These properties make it ideal for LED encapsulation [83].

Silicone is known for its high transmittance with a relatively good thermal stability, which is another option to build low-loss optical systems [84, 85]. Sylgard 3-6636 was first considered because it is a silicone-based material, but its supply had been discontinued in the beginning of this study. EI-1184 silicone polydimethylsiloxane (PDMS) elastomer encapsulant is an alternative of 3-6636, due to its similar physical properties. Typical silicone rubber has thermal conductivity of 0.20 W/m K [86]. EI-1184 has a RI of 1.42 at 632.8 nm [87]. It also has remarkable properties such as good thermal stability, corrosion resistance, flexibility, high purity, and high transparency, which could make it an excellent choice for UV-C LED encapsulation [58, 87-90].

According to the datasheet provided by the supplier, EI-1184 has additional features such as reduced yellowing for longer device lifetime, and outstanding transparency at 380 nm [87]. Fig. 18 provides the transmittance of EI-1184 with a thickness of 3.2 mm at 380 nm, 450 nm, and 760 nm. However, the transmittance under 380 nm has not been investigated. This is studied in this thesis, and the results will be discussed in the Chapter 5.

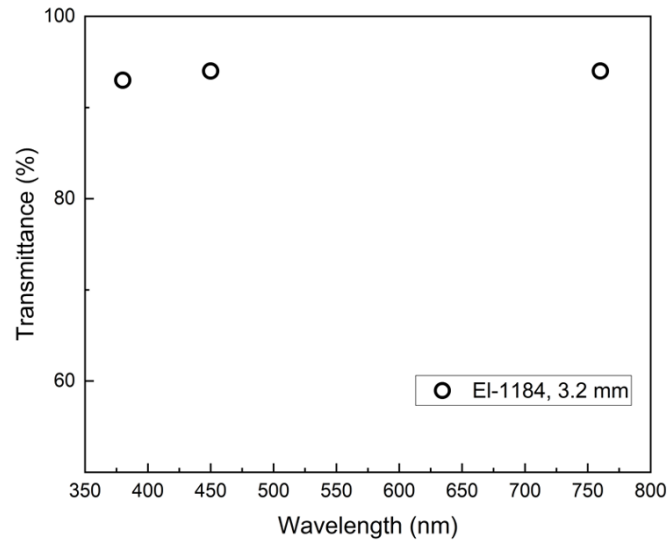


Figure 18: Transmittance of EI-1184 with a thickness of 3.2 mm [87].

CHAPTER 5

Encapsulation Results

In Chapter 3, the mounting process of LED die to TO-39 header has been described. In Chapter 4, the design considerations of encapsulation have been discussed. In this chapter, the results of encapsulation will be discussed. Section 5.1 describes the polymer curing process and the transmittance results of cured UR5638 and EI-1184 epoxy resins, followed by Section 5.2 that shows the results of the mounted nanowire DUV LED die after encapsulation.

5.1 Curing Process and Transmittance

5.1.1 UR5638

The top row of Fig. 19 shows the cured UR5638 resins with different thicknesses of 1 mm, 1.2 mm, 1.5 mm, and 2 mm. The epoxy resins were prepared on microscope glass slides at room temperature and peeled off once they were cured. The curing time is around 24 hours. The resin samples were then cut into smaller pieces which later serve for the transmittance test.

The bottom row of Fig. 19 shows the cured epoxy resins in dome shape. In contrast with flat shape encapsulation, high curing temperatures were used so that different dome shapes can be formed, due to the different degree of surface tension relaxation at different temperatures. As such, the dome shapes are self-organized. The temperature was controlled by setting up an oven. Curing time and duration up to 4 hours and 60 °C were used, respectively. As shown in the Fig. 19, domes with different heights of 1 mm, 2 mm, 2.5 mm, and 3 mm were obtained. These height values correspond to the height to radius ratios of 0.2, 0.5, 0.6, and 1.

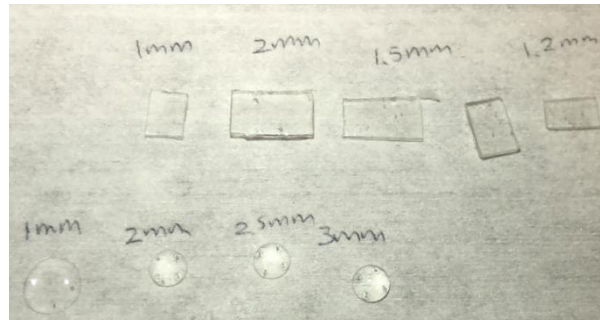


Figure 19: Cured UR5638 resins.

The transmittance was then measured with a 266 nm laser beam, which was generated by the 2nd harmonic of a green laser. To control the laser beam shape as well as to minimize the unwanted green light, a pinhole was used. Photodetector was used to measure the light intensity of the laser beam before and after passing through the cured material. As such, transmittance was estimated by the ratio of the incident laser beam intensity to the transmitted laser beam intensity. It is found that the transmittance decreases as the thickness increases; while for the dome shapes, there is a tendency of increasing transmittance as the height to radius ratio increases. Nonetheless, a maximum transmittance of only 4.4% was obtained regardless of the shapes, indicating that UR5638 is not suitable for DUV LED Encapsulation.

5.1.2 EI-1184

As no significant difference was seen comparing dome shape and other cured shapes (mainly rectangular shapes) for UR5638, near-rectangular shapes were used for EI-1184 transmittance test, due to the simplicity in processing such shapes. Shown in Fig. 20 is a photo of cured EI-1184 resins with different thicknesses (e.g., 0.25 mm, 0.5 mm, 0.75 mm, and 1 mm). The near-rectangular shapes were obtained following the procedure described earlier for UR5638.

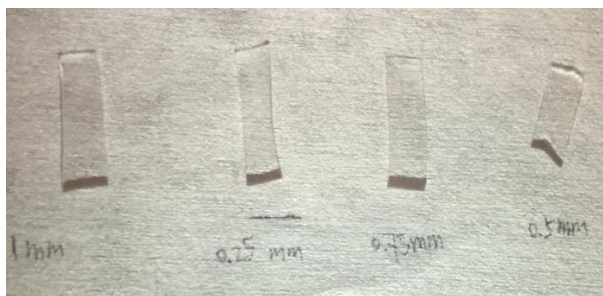


Figure 20: Cured EI-1184 resins.

The measured transmittance as a function of the thickness is shown in Fig. 21. It is seen that, as the thickness increases, the transmittance reduces. However, a maximum transmittance of 92.8% can be obtained for a thin layer. This suggests that EI-1184 could be a choice for UV-C LED Encapsulation. Moreover, it is also noted that, besides this high transmittance, as a family member of silicone-based materials, EI-1184 also exhibits good thermal stability, UV resistance, flexibility, corrosion resistance and high RI (as mentioned earlier in Section 4.2). Therefore, EI-1184 is a promising material for DUV LED encapsulation.

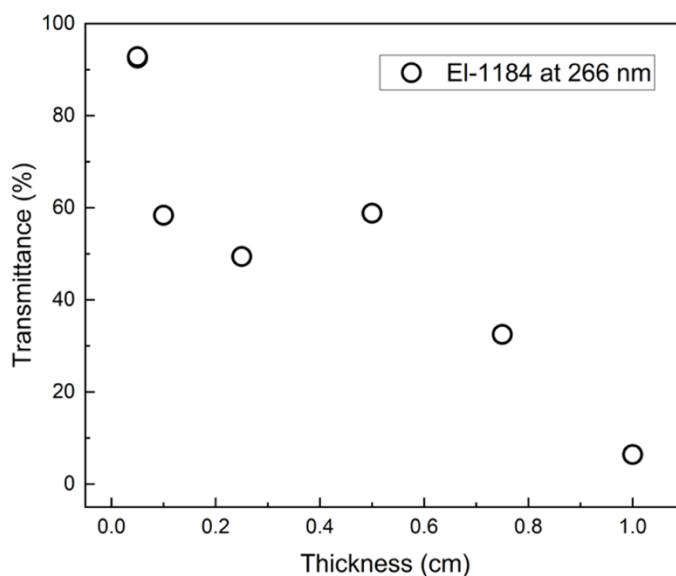


Figure 21: Transmittance of bare EI-1184.

5.1.3 Tools and Materials for Curing and Transmittance Measurement

Table 2: List of materials and tools for curing and transmittance measurement

Baking Tools	
Fisher Scientific 3510Fs gravity oven	1 unit
Glass slide	multiple
Epoxy Resins	
UR5638 polyurethane resin	2 × 210 ml
DOWSIL EI-1184 gel	5 × 210 ml
Transmittance Measurement Tools	
266 nm laser	1 unit
NEWPORT 843-R-USB photodetector	1 unit

5.2 Encapsulation of AlGaN Nanowire DUV LED Die on TO-header

A photograph of an encapsulated LED chip is shown below in Fig. 22, which includes an LED die containing a $1 \times 1 \text{ mm}^2$ AlGaN nanowire DUV LED, which is mounted to a TO-39 header, and further encapsulated with EI-1184.



Figure 22: Image of encapsulated AlGaN nanowire DUV LED die.

Similar to the measurement of LOP of bare AlGaIn nanowire DUV LEDs, a Si-based photodetector was used to measure the LOP of the mounted LED devices before and after encapsulation. Breadboard (also shown in Fig. 22) was used to connect the LED chip with the positive and negative terminals of the current source. In this experiment, the same measurement condition was applied to the LED die before and after encapsulation. The measured LOP before encapsulation and after encapsulation give a ratio around 80%, indicating that the encapsulation process does not significantly degrade the performance of the LED. A further and more strict comparison on LOP can be carried out by using an integration sphere, which is one of the future studies as discussed in Chapter 7.

The materials and tools used in the encapsulation process are listed in the end in the table below.

Table 3: List of materials and tools for encapsulation

Encapsulants	
DOWSIL EI-1184 gel	5 × 210 ml
Encapsulation Tools	
3 ml syringe	multiple
1 Inch 18G blunt tip syringe needles	100 pieces
LED die on TO-39 header	multiple
Gloves for Protection	multiple

CHAPTER 6

Disinfection Experiments

The disinfection effect of AlGa_N nanowire DUV LEDs is investigated in this chapter. Human Coronavirus 229E (HCoV-229E) is used in this regard. As a species of coronavirus, it brings special interests because of the ongoing pandemic at the time of writing this thesis. Disinfection experiments on bare AlGa_N nanowire DUV LEDs are first discussed in Section 6.1, followed by the progress on disinfection experiments using AlGa_N nanowire DUV LED wafers covered with EI-1184 in Section 6.2.

6.1 Disinfection Experiments on Bare AlGa_N Nanowire DUV LEDs

The reason why encapsulant was not used in the this set of experiments was because there was not much prior information on such experiments, and the goal for this set of experiments was to obtain some basic disinfection properties, which can be used for later experiments.

6.1.1 Setup

The setup shown in Fig. 23 was carried to Dr. Liang's medical science research lab. Easy transportation and the ability to provide stable LED device electrical connection have been taken into consideration of designing such a setup. In this setup, source meter is used to supply current to LED devices. A metal plate is used to hold the wafer and to conduct current from the positive terminal to the devices. Thin bonding wires are used to connect the negative terminal to the metal contact of the LED devices. Liquid-based colloidal Ag paste is used in the connection between the bonding wires and the electrical cable to the negative terminal to enhance the electrical conduction.

Moreover, the setup needs to be placed on an isolated and flat surface such as wood, glass, and plastic.

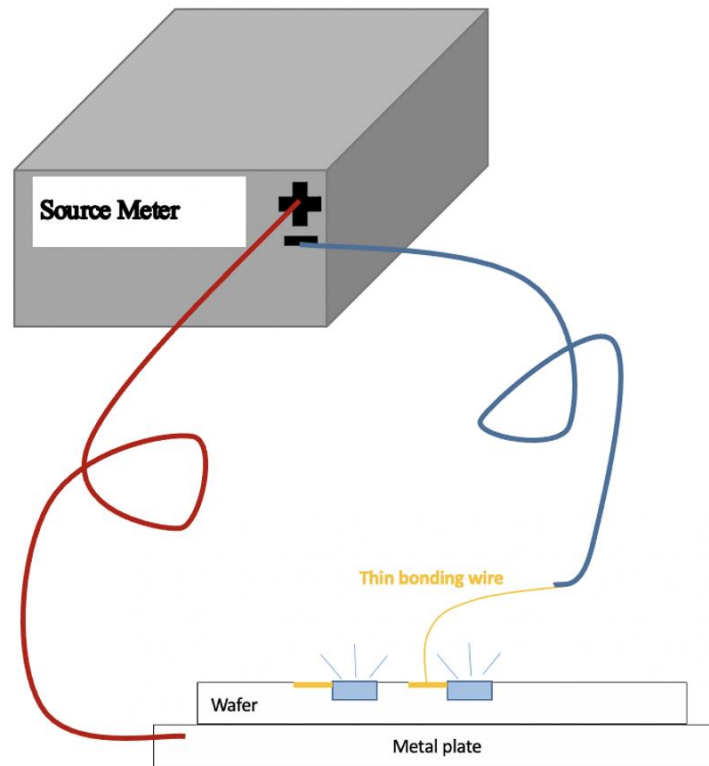


Figure 23: Schematic of the circuit setup.

6.1.2 Virus Placement

Because HCoV-229E viruses are infectious, the materials and surfaces that have direct contact with the viruses need to be sterilized completely by ethanol or other types of sterilization chemicals after each use. To prevent the surface of the LED device from being damaged by sterilization, a material that is transparent, disposable, and water resistant is required in the setup to place the viruses.

In this thesis study, there are many materials that have been considered and tested for the virus placement, such as microscope glass slide, plastic petri dish, and so on. Among various

candidates, microscope glass slide could be the choice, which meets the experiment requirement and has a transmittance of 20%, which is low but higher than other candidates.

The virus placement is illustrated in Fig. 24. 5 μL of virus media is used for each test. The distance between the media and the LED devices is 4.5 cm. Two holders are used to stabilize the glass slide. In this way, the media containing viruses can be easily deposited and retrieved. The glass slide can also be disposed of and replaced after each use to meet the medical safety requirements.

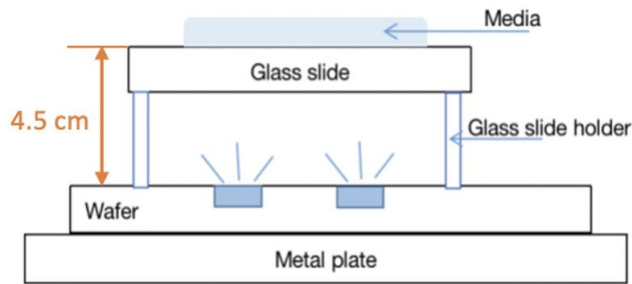


Figure 24: Schematic of the setup for disinfection experiments with non-encapsulated AlGaIn nanowire DUV LED wafers.

6.1.3 Experimental Condition Estimation

Before the experiments, it is important to estimate how long the UV irradiation of the AlGaIn nanowire DUV LEDs is required to inactivate HCoV-229E virus based on the known data and references. From Eq. 4, time is determined by the energy required to kill viruses and the LOP of the LED chip.

$$Time = \frac{Energy}{Power} \quad (4)$$

UV dose is a measure of energy required for disinfection. There is no information found that specifies the amount of UV dose required to inactivate HCoV-229E virus. UV data sheet from ClorDiSys provides different UV doses required to inactivate a list of known bacteria [91]. By

referencing the average UV dose for bacteria, an energy of 50 mJ was assumed to disinfect a 1 cm² surface area for intended used virus [91]. However, it is noted that genetic information in bacteria is encoded in DNA, which is more UV sensitive than RNA encoded coronavirus [14, 92].

Another assumption was on the surface area that 5 μL of virus media can cover. Fig. 25 provides an illustration of the surface area that a water drop can cover on glass with respect to volume. Because the media is simply water with additional nutrient ingredients, the volume and surface area presented in Fig. 25(a) for water are used as a reference for the virus media in this study. For 5 μL of virus media, a surface area of 2.5 mm² can be covered on glass. Therefore, the required energy is 1.25 mJ to disinfect a surface of 2.5 mm².

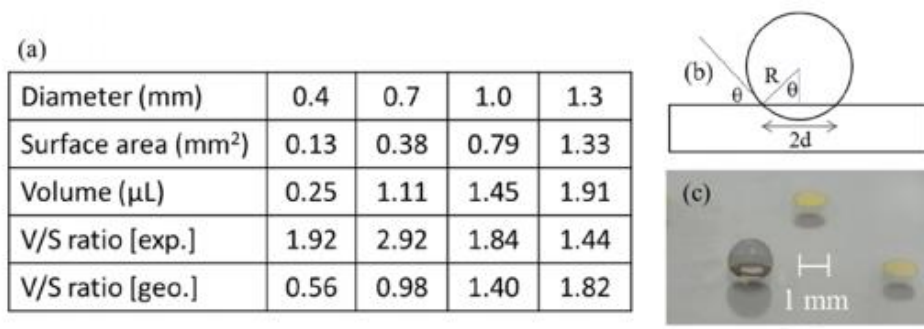


Figure 25: Illustration of the relation between volume and surface area for water. (a) Table of spot surface area, volume, diameter, volume to surface area ratio from experiment and geometrically derived. (b) Marked sketch of cross section. (c) Image of 1.5 μL water on glass surface [93].

For the LOP of AlGa_N nanowire DUV LEDs, it depends on the applied current. Referring to Fig. 10 for the LOP of a 1 × 1 mm² AlGa_N nanowire DUV LED, when applied current is 5 mA, LOP is approximately 5 μW, and LOP increases to 10 μW with 10 mA of applied current. However, the power loss from the glass slide needs to be considered. Therefore, LOP after glass slide are 1 μW at 5 mA and 2 μW at 10 mA, respectively.

As such, disinfection time of 1250 seconds (~20 minutes) is required to be effective for an applied current of 5 mA. Similarly, 625 seconds (~10 minutes) are required at 10 mA. These estimations provide a guidance for the disinfection experiments.

6.1.4 Experimental Procedure

Experimentally, media containing HCoV-229E virus was always retrieved and deposited in triplicate after UV irradiation. Then, to measure whether the retrieved virus was infectious or not, Huh7 cell was used as a test, which is a human liver cell line that is permissive to HCoV-229E infection. In this regard, relative luminescence unit (RLU), which indicates the amount of virus replication in the infected cells, was measured, to evaluate whether virus was infectious or not (i.e., whether Huh7 cell was infected by the virus). Low infectious viruses (less replication activities in cells) give low RLU counts, and viruses that are highly infectious give higher RLU counts. In this experiment, RLU was measured for samples related to different UV irradiation time (e.g., 0 min, 1 min, etc.).

6.1.5 Results

This section presents the results of disinfection experiments. The results of control experiments are described first, followed by the disinfection results. UV light from daylight and room light has been minimized during the experiments and is further considered in the control experiments.

a) Control Experiments

Control experiments are important to test the impact of background noise such as UV light from daylight and room light. In this study, control experiments without DUV irradiation from

AlGaN nanowire DUV LEDs were performed. The RLU results are illustrated in Fig. 26. It is seen that average RLU values fluctuate around 80,000 and are time independent, suggesting that without UV irradiation from the AlGaN nanowire DUV LEDs, there are no disinfection effects.

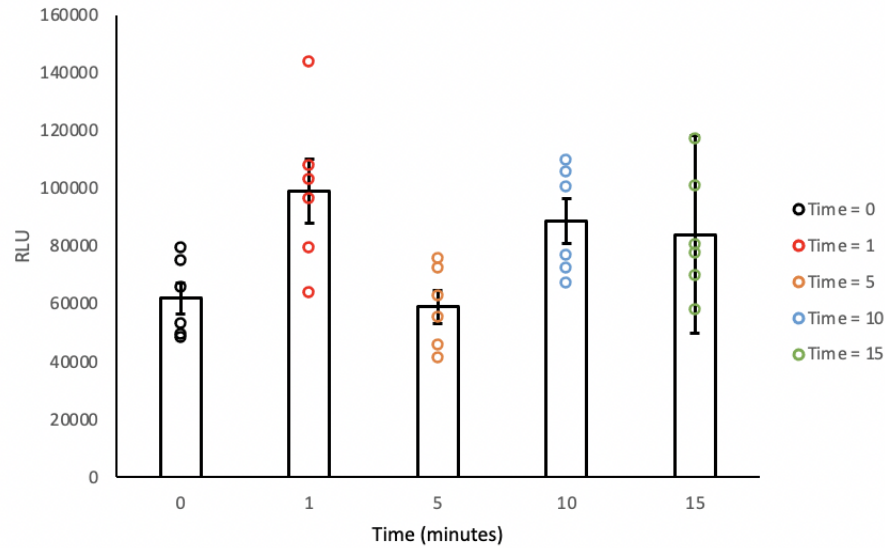


Figure 26: RLU as a function of time without UV-C irradiation from AlGaN nanowire DUV LEDs.

b) Disinfection Experiments

Fig. 27 and Fig. 28 present the inactivation results from a single $1 \times 1 \text{ mm}^2$ AlGaN nanowire DUV LED at disinfection time of 0 min, 1 min, 5 min, 10 min, and 15 min. Under the consideration of real-life intended use, disinfection time up to 15 minutes was decided to investigate the virus inactivation effect in a short period of time. Fig. 27(a) shows the RLU results as a function of time with 5 mA applied current. The minimum RLU occurs at 10 minutes and the infectivity decreases to 17.25% as shown in Fig. 27(b). The infectivity was calculated by taking the average RLU value after DUV irradiation over the average RLU value at time 0. Inactivation efficiency is the reverse of the infectivity, which is thus 82.75%.

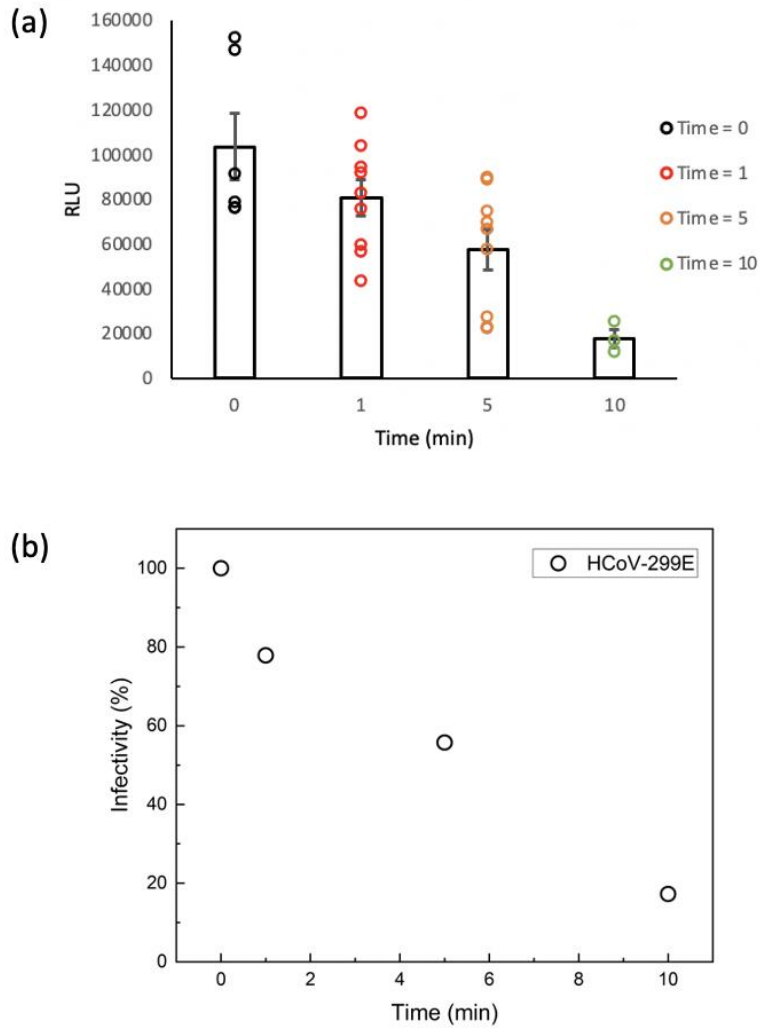


Figure 27: (a) RLU and (b) infectivity as a function of time with 5 mA applied current.

Fig. 28(a) shows the mean RLU results as a function of time with 10 mA applied current. The minimum RLU occurs at 15 minutes and the infectivity decreases to 8.72% as shown in Fig. 28(b). 91.28% of viral inactivation efficiency is thus obtained. There is a significant reduction of RLU and infectivity under the UV irradiation from single AlGaIn nanowire DUV LEDs.

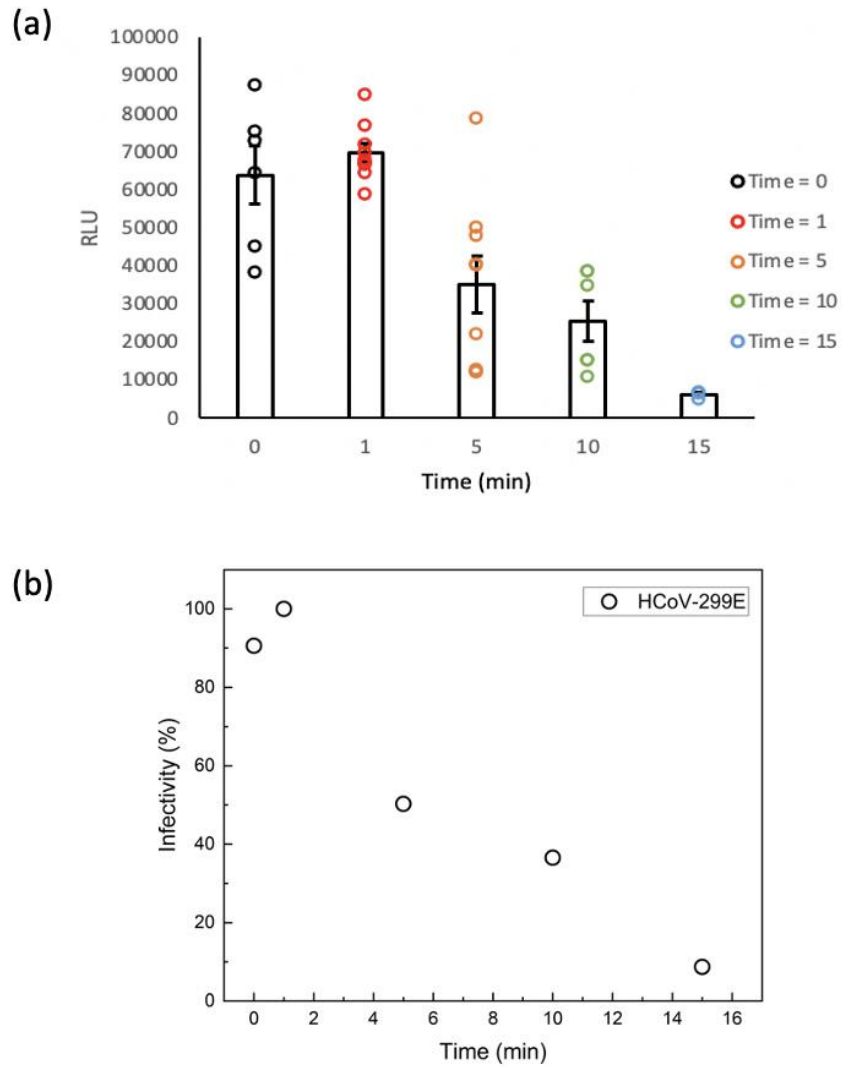


Figure 28: (a) RLU and (b) infectivity with respect to time with 10 mA applied current.

R-Log reduction is generally used to describe the disinfection response and can be calculated as Eq. 5:

$$R = -\log_{10}\left(\frac{N_a}{N_b}\right) \quad (5)$$

whereas N_b and N_a are the infectivity of the virus sample before and after the UV irradiation treatment. In this study, maximum R-log reduction of 1 log₁₀ is achieved with 10 mA of applied current at 15 minutes.

6.1.6 Tools and Materials

Table 4: List of materials and tools for disinfection experiments

LED Wafer Setup Tools	
AlGaIn nanowire DUV LED wafer	multiple
Keithley source meter	1 unit
Tweezers	1 pair
Metal plate	2
Disinfection Test Tools	
Glass slide	multiple
Glass slide holder	2 nut pairs
Syringe	multiple
Nutrient media containing viruses	5 μ L for each time point
Nutrient media for retrieving purposes	10 μ L for each time point

6.2 Disinfection Experiments on AlGaIn Nanowire DUV LEDs Covered with EI-1184

Based on the study in Section 6.1, it is necessary to remove glass slides as one way to improve the inactivation efficiency. As EI-1184 can be used for virus placement directly, AlGaIn nanowire DUV LEDs can be covered by EI-1184 in a flat shape with improved DUV light transmittance. Namely, comparing to using microscope glass slides, this can significantly reduce the wasted photons due to the low transmittance of microscope glass slides, and thus improves inactivation efficiency. This is schematically shown in Fig. 29. The distance between the virus-containing media and the device top surface can be further controlled by the thickness of the polymer layer.

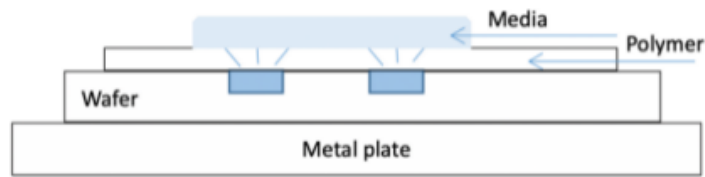


Figure 29: Schematic of disinfection test setup with encapsulant.

It is further noted that, such a flat shape is not only to provide a suitable experimental setting and a protection layer for LED devices, but also to mimic the real-life intended use such as touch screen display, wherein the contact is a flat surface.

Experimentally, considering the surface tension, the sample would suffer from the uneven surface such as the center of the surface would hump. A flat shape might not be achieved when applying to a small area. Moreover, with a higher curing temperature, the curing process accelerates, so that the surface tension of the encapsulant cannot be relaxed, due to the high viscosity of the material, leading to a non-flat surface.

To overcome this issue, in this thesis study, EI-1184 was applied on a relatively large surface area ($\sim 50 \text{ mm} \times 50 \text{ mm}$) and was cured at the room temperature. Cure time of at least 4 hours was used. Moreover, a thin layer with a thickness of 0.1 cm or less was used, in order to maintain a relatively high transmittance. Multiple $1 \times 1 \text{ mm}^2$ LED devices were wire bonded before applying EI-1184. The AlGaIn nanowire DUV LED wafer covered with cured EI-1184 is shown in Fig. 30. It is seen that a large area near flat surface that contains a number of bonded AlGaIn nanowire DUV LEDs is obtained. The LED devices were further tested by probing after applying EI-1184, and it was found that the encapsulation process did not affect the electrical connection of the LED devices.

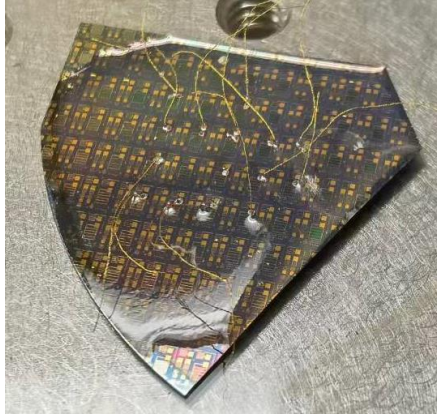


Figure 30: Image of AlGaIn nanowire DUV LED wafer covered by EI-1184 in a near flat shape.

CHAPTER 7

Conclusions and Future Work

In this thesis, the packaging and disinfection effect of AlGaN nanowire DUV LEDs are investigated. TO-39 header is used to mount the LED die, and two different polymers are tested. It is found that EI-1184 has an excellent transmittance in the DUV range and is used subsequently for the encapsulation after mounting the LED die onto the TO-header. Regarding to the disinfection effect, bare AlGaN nanowire DUV LEDs are tested as the starting point, 1 log₁₀ R-log reduction is achieved from a single 1 × 1 mm² AlGaN nanowire DUV LED. Moreover, to accommodate the disinfection experiments for the next step, encapsulation of devices without using TO-header is studied. In this regard, multiple devices on a large wafer are directly covered by EI-1184, and flat shape has been obtained by controlling the curing condition.

In this thesis study, the inactivation efficiency has remained low. According to the “ARCHIVED Guidance document - Safety and efficacy requirements for hard surface disinfectant drugs” published by Health Canada, “A minimum recoverable endpoint viral titer after drying of 4 log₁₀ is required” for disinfectants used against viruses [94]. The following strategies can be used to further improve the inactivation efficiency.

First of all, in the present disinfection experiments, single 1 × 1 mm² devices were used. Naturally, to enhance the inactivation efficiency, an array of devices can be used. In this regard, multiple devices can be connected in parallel and turned on simultaneously. Such a system could be potentially powered up by batteries.

Furthermore, as mentioned in Chapter 6, AlGaN nanowire DUV LEDs covered with EI-1184 in a flat shape could also improve the inactivation efficiency, due to the improved light transmission.

Moreover, a fundamental improvement on the inactivation efficiency can be achieved by further engineering the AlGaN nanowire DUV LEDs used in the present study. For example, the I-V characteristics of such devices indicate the presence of large series resistance, which could be potentially alleviated by further improving the doping in the p-type AlGaN layer, improving the design of the device structure, and so on. It is also noted that, although EI-1184 is found to be an excellent encapsulant in the DUV range, the detailed investigation of the LOP after encapsulating the LED die on TO-header is required, such as the shape versus LOP for packaged devices. This can be done by using integration sphere. A full understanding of the LOP of packaged devices can possibly improve inactivation efficiency as well. Lastly, engineering the device emission wavelength by changing Al and Ga composition can also possibly improve the inactivation efficiency.

References

1. Norval, M., et al., *The effects of ultraviolet light irradiation on viral infections*. British Journal of Dermatology, 1994. **130**(6): p. 693-700.
2. Svobodova, A., D. Walterova, and J. Vostalova, *Ultraviolet light induced alteration to the skin*. Biomedical Papers-Palacky University in Olomouc, 2006. **150**(1): p. 25.
3. Song, K., M. Mohseni, and F. Taghipour, *Application of ultraviolet light-emitting diodes (UV-LEDs) for water disinfection: A review*. Water research, 2016. **94**: p. 341-349.
4. Gayán, E., C. Santiago, and Á. Ignacio, *Biological aspects in food preservation by ultraviolet light: a review*. Food and Bioprocess Technology, 2014. **7**(1): p. 20.
5. Ulm, R. and F. Nagy, *Signalling and gene regulation in response to ultraviolet light*. Current opinion in plant biology, 2005. **8**(5): p. 477-482.
6. Ensminger, P.A., *Control of development in plants and fungi by far - UV radiation*. Physiologia Plantarum, 1993. **88**(3): p. 501-508.
7. Hsu, T.-C., et al. *Perspectives on UVC LED: Its progress and application*. in *Photonics*. 2021. Multidisciplinary Digital Publishing Institute.
8. Hessling, M., et al., *The impact of far-UVC radiation (200–230 nm) on pathogens, cells, skin, and eyes—a collection and analysis of a hundred years of data*. GMS Hygiene and Infection Control, 2021. **16**.
9. Hockberger, P.E., *A History of Ultraviolet Photobiology for Humans, Animals and Microorganisms*. Photochemistry and photobiology, 2002. **76**(6): p. 561-579.
10. Linden, K.G., N. Hull, and V. Speight, *Thinking outside the treatment plant: UV for water distribution system disinfection*. Accounts of Chemical Research, 2019. **52**(5): p. 1226-1233.
11. Shah, J., A. Židonis, and G. Aggidis, *State of the art of UV water treatment technologies and hydraulic design optimisation using computational modelling*. Journal of Water Process Engineering, 2021. **41**: p. 102099.
12. Organization, W.H., *Coronavirus disease (COVID-19) pandemic*. 2022: www.who.int.
13. Woo, P.C., et al., *Discovery of seven novel Mammalian and avian coronaviruses in the genus deltacoronavirus supports bat coronaviruses as the gene source of alphacoronavirus and betacoronavirus and avian coronaviruses as the gene source of*

- gammacoronavirus and deltacoronavirus*. Journal of virology, 2012. **86**(7): p. 3995-4008.
14. Fehr, A.R. and S. Perlman, *Coronaviruses: an overview of their replication and pathogenesis*. Coronaviruses, 2015: p. 1-23.
 15. Giwa, A. and A. Desai, *Novel coronavirus COVID-19: an overview for emergency clinicians*. Emerg Med Pract, 2020. **22**(2 Suppl 2): p. 1-21.
 16. V'kovski, P., et al., *Coronavirus biology and replication: implications for SARS-CoV-2*. Nature Reviews Microbiology, 2021. **19**(3): p. 155-170.
 17. Ong, Q., et al., *Irradiation of UVC LED at 277 nm inactivates coronaviruses by photodegradation of spike protein*. bioRxiv, 2021.
 18. Krammer, F., *SARS-CoV-2 vaccines in development*. Nature, 2020. **586**(7830): p. 516-527.
 19. Amanat, F. and F. Krammer, *SARS-CoV-2 vaccines: status report*. Immunity, 2020. **52**(4): p. 583-589.
 20. Sommerstein, R., et al., *Risk of SARS-CoV-2 transmission by aerosols, the rational use of masks, and protection of healthcare workers from COVID-19*. Antimicrobial Resistance & Infection Control, 2020. **9**(1): p. 1-8.
 21. Organization, W.H., *Coronavirus disease (COVID-19): Cleaning and disinfecting surfaces in non-health care settings*, in *Newroom*. 2020: www.who.int.
 22. Noorimotlagh, Z., et al., *A systematic review of emerging human coronavirus (SARS-CoV-2) outbreak: focus on disinfection methods, environmental survival, and control and prevention strategies*. Environmental Science and Pollution Research, 2021. **28**(1): p. 1-15.
 23. Raeiszadeh, M. and B. Adeli, *A critical review on ultraviolet disinfection systems against COVID-19 outbreak: Applicability, validation, and safety considerations*. Acs Photonics, 2020. **7**(11): p. 2941-2951.
 24. Bormann, M., et al., *Disinfection of SARS-CoV-2 contaminated surfaces of personal items with UVC-LED disinfection boxes*. Viruses, 2021. **13**(4): p. 598.
 25. Perdiz, D., et al., *Distribution and repair of bipyrimidine photoproducts in solar UV-irradiated mammalian cells: possible role of Dewar photoproducts in solar mutagenesis*. Journal of Biological Chemistry, 2000. **275**(35): p. 26732-26742.

26. Ravanat, J.-L., T. Douki, and J. Cadet, *Direct and indirect effects of UV radiation on DNA and its components*. Journal of Photochemistry and Photobiology B: Biology, 2001. **63**(1-3): p. 88-102.
27. Zavestovskaya, I.N., et al., *Inactivation of coronaviruses under irradiation by UVA-range light-emitting diodes*. Quantum Electronics, 2022. **52**(1): p. 83.
28. Darnell, M.E., et al., *Inactivation of the coronavirus that induces severe acute respiratory syndrome, SARS-CoV*. Journal of virological methods, 2004. **121**(1): p. 85-91.
29. Kebbi, Y., et al., *Recent advances on the application of UV - LED technology for microbial inactivation: Progress and mechanism*. Comprehensive Reviews in Food Science and Food Safety, 2020. **19**(6): p. 3501-3527.
30. Chiappa, F., et al., *The efficacy of ultraviolet light-emitting technology against coronaviruses: a systematic review*. Journal of Hospital Infection, 2021. **114**: p. 63-78.
31. Gerchman, Y., et al., *UV-LED disinfection of Coronavirus: Wavelength effect*. Journal of Photochemistry and Photobiology B: Biology, 2020. **212**: p. 112044.
32. Minamikawa, T., et al., *Quantitative evaluation of SARS-CoV-2 inactivation using a deep ultraviolet light-emitting diode*. Scientific Reports, 2021. **11**(1): p. 1-9.
33. Kessler, R., *The Minamata Convention on Mercury: a first step toward protecting future generations*. 2013, National Institute of Environmental Health Sciences.
34. Heering, W., *UV sources—basics, properties and applications*. IUVA news, 2004. **6**(4): p. 7-13.
35. Chen, J., S. Loeb, and J.-H. Kim, *LED revolution: fundamentals and prospects for UV disinfection applications*. Environmental Science: Water Research & Technology, 2017. **3**(2): p. 188-202.
36. Vincent C., F. *Understanding Ultraviolet LED Applications and Precautions*. 2014 2022 [cited 2022 January 15]; Available from: <https://marktechopto.com/technical-articles/understanding-ultraviolet-led-applications-and-precautions/>.
37. Amano, H., et al., *The 2020 UV emitter roadmap*. Journal of Physics D: Applied Physics, 2020. **53**(50): p. 503001.
38. Berneburg, M., M. Röcken, and R. Benedix, *Phototherapy with narrowband UVB*. Acta Derm Venereol, 2005. **85**: p. 1-11.

39. Laura, W., *Global Ultraviolet (UV) LED Market Report 2020-2025 - Sterilization to Significantly Contribute to Market Growth*. 2020, Globe Newswire: ResearchAndMarkets.com.
40. Liang, S. and W. Sun, *Recent Advances in Packaging Technologies of AlGaN - Based Deep Ultraviolet Light - Emitting Diodes*. *Advanced Materials Technologies*, 2022: p. 2101502.
41. Lei, W.-S., A. Kumar, and R. Yalamanchili, *Die singulation technologies for advanced packaging: A critical review*. *Journal of Vacuum Science & Technology B, Nanotechnology and Microelectronics: Materials, Processing, Measurement, and Phenomena*, 2012. **30**(4): p. 040801.
42. Zhong, Z.-W., *Advanced polishing, grinding and finishing processes for various manufacturing applications: a review*. *Materials and Manufacturing Processes*, 2020. **35**(12): p. 1279-1303.
43. Peng, Y., et al., *Progress and perspective of near-ultraviolet and deep-ultraviolet light-emitting diode packaging technologies*. *Journal of Electronic Packaging*, 2019. **141**(4).
44. Alim, M.A., et al., *Die attachment, wire bonding, and encapsulation process in LED packaging: A review*. *Sensors and Actuators A: Physical*, 2021. **329**: p. 112817.
45. Lee, S., et al., *Emerging trend for LED wafer level packaging*. *Frontiers of Optoelectronics*, 2012. **5**(2): p. 119-126.
46. Weerasinghe, H.C., et al., *Encapsulation for improving the lifetime of flexible perovskite solar cells*. *Nano Energy*, 2015. **18**: p. 118-125.
47. Luo, X. and R. Hu, *Chip packaging: Encapsulation of nitride LEDs*, in *Nitride semiconductor light-emitting diodes (LEDs)*. 2014, Elsevier. p. 441-481.
48. Hu, J., L. Yang, and M.W. Shin, *Mechanism and thermal effect of delamination in light-emitting diode packages*. *Microelectronics Journal*, 2007. **38**(2): p. 157-163.
49. Hu, J., L. Yang, and M.W. Shin. *Thermal effects of moisture inducing delamination in light-emitting diode packages*. in *56th Electronic Components and Technology Conference 2006*. 2006. IEEE.
50. Luo, X., B. Wu, and S. Liu, *Effects of moist environments on LED module reliability*. *IEEE Transactions on device and materials reliability*, 2009. **10**(2): p. 182-186.

51. Lu, Y., et al., *Zirconia/phenylsiloxane nano-composite for LED encapsulation with high and stable light extraction efficiency*. RSC Advances, 2021. **11**(30): p. 18326-18332.
52. Loctite, *Technical Data Sheet HYSOL OS4000*. 2002.
53. LED, C., *SLamp XP-G3 LEDs*, Cree, Editor. 2016.
54. Lin, Y.-C., et al., *LED and optical device packaging and materials*, in *Materials for advanced packaging*. 2009, Springer. p. 629-680.
55. Yu, H.-x., et al., *Surface chemical changes analysis of UV-light irradiated Moso bamboo (Phyllostachys pubescens Mazel)*. Royal Society open science, 2018. **5**(6): p. 180110.
56. Chris, R., *UV Degradation Effects in Materials - An Elementary Overview*, in *UV Solutions*. 2019.
57. Silicone, S.-E., *What is silicone made of?*, in *What is silicone? : Learn more about silicones*.
58. Lin, Y.-H., et al., *Development of high-performance optical silicone for the packaging of high-power LEDs*. IEEE Transactions on Components and Packaging Technologies, 2010. **33**(4): p. 761-766.
59. Moustakas, T.D. and R. Paiella, *Optoelectronic device physics and technology of nitride semiconductors from the UV to the terahertz*. Reports on Progress in Physics, 2017. **80**(10): p. 106501.
60. Hirayama, H., S. Fujikawa, and N. Kamata, *Recent progress in AlGaIn - based deep - UV LEDs*. Electronics and Communications in Japan, 2015. **98**(5): p. 1-8.
61. Fujita, S., *Wide-bandgap semiconductor materials: For their full bloom*. Japanese journal of applied physics, 2015. **54**(3): p. 030101.
62. Shur, M.S. and R. Gaska, *Deep-ultraviolet light-emitting diodes*. IEEE Transactions on electron devices, 2009. **57**(1): p. 12-25.
63. Sadaf, S., et al., *An AlGaIn core-shell tunnel junction nanowire light-emitting diode operating in the ultraviolet-C band*. Nano letters, 2017. **17**(2): p. 1212-1218.
64. Glas, F., *Critical dimensions for the plastic relaxation of strained axial heterostructures in free-standing nanowires*. Physical Review B, 2006. **74**(12): p. 121302.
65. Zhao, S., et al., *AlGaIn nanowires for ultraviolet light-emitting: recent progress, challenges, and prospects*. Micromachines, 2020. **11**(2): p. 125.

66. Fang, Z., et al., *Si donor incorporation in GaN nanowires*. Nano letters, 2015. **15**(10): p. 6794-6801.
67. Zhao, S., et al., *Aluminum nitride nanowire light emitting diodes: Breaking the fundamental bottleneck of deep ultraviolet light sources*. Scientific reports, 2015. **5**(1): p. 1-5.
68. Zhao, S., et al., *p-Type InN nanowires*. Nano letters, 2013. **13**(11): p. 5509-5513.
69. Paschotta, R., *Encyclopedia of laser physics and technology*. Vol. 1. 2008: Wiley-vch.
70. Fu, H. and Y. Zhao, *Efficiency droop in GaInN/GaN LEDs*, in *Nitride semiconductor light-emitting diodes (LEDs)*. 2018, Elsevier. p. 299-325.
71. Engineering R&D Division, E.S.D., Accessory Equipment Group, *Usefulness of the ultra-compact deionized water recycling unit for dicing saws*, DISCO, Editor. 2016.
72. UKAM, *DICING BLADE OPERATION RECOMMENDATIONS*. 2009: ukam.com.
73. Gan, Y., X. Jiang, and J. Yin, *Thiol-ene photo-curable hybrid silicone resin for LED encapsulation: enhancement of light extraction efficiency by facile self-keeping hemisphere coating*. Journal of Materials Chemistry C, 2014. **2**(28): p. 5533-5539.
74. Consonni, M., et al., *Combined experimental and Monte-Carlo ray-tracing approach for optimizing light extraction in LED COB modules*. International Scholarly Research Notices, 2013. **2013**.
75. Moulin, G., et al., *An Efficient Process of Surface Modification and Patterning for LED Encapsulation*. IEEE Transactions on Components, Packaging and Manufacturing Technology, 2018. **8**(5): p. 904-909.
76. Wu, S., et al., *Enhanced light extraction efficiency of UV LEDs by encapsulation with UV-transparent silicone resin*. Semiconductor Science and Technology, 2022.
77. Steven, K. *Improving the Efficiency of LED Light Emission*. [online article] 2011-2021-08-09 [cited 2022 January 15]; Available from: <https://www.digikey.com/en/articles/techzone/2011/aug/improving-the-efficiency-of-led-light-emission>.
78. E. Fred, S., *Materials Refractive Index and Extinction Coefficient*. 2004.
79. Sun, Y., et al., *Oligo-fluoropolymer Modified Cycloaliphatic Epoxy Resins with Excellent Compatibility, Waterproof and Mechanical Properties for LED Encapsulation*. Chemical Research in Chinese Universities, 2018. **34**(2): p. 326-332.

80. Lin, C.-H., et al., *Novel siloxane-modified epoxy resins as promising encapsulant for LEDs*. *Polymers*, 2019. **12**(1): p. 21.
81. Tao, P., et al., *Transparent dispensible high - refractive index ZrO₂/epoxy nanocomposites for LED encapsulation*. *Journal of Applied Polymer Science*, 2013. **130**(5): p. 3785-3793.
82. ToolBox, E., *Air - Thermal Conductivity vs. Temperature and Pressure*. 2009.
83. Alistair, L., *Polyurethane encapsulants offer enhanced protection for LEDs in challenging environments*, in *LEDs Magazine*. 2019.
84. Jayawardena, A. and N. Narendran, *Analysis of electrical parameters of InGaN-based LED packages with aging*. *Microelectronics Reliability*, 2016. **66**: p. 22-31.
85. Chung, P.T., et al., *ZrO₂/epoxy nanocomposite for LED encapsulation*. *Materials Chemistry and Physics*, 2012. **136**(2-3): p. 868-876.
86. intertronics, *Thermally Conductive Silicones*. 2018.
87. Company, T.D.C., *DOWSIL EI-1184 Optical Encapsulant*, Dow, Editor. 2018: www.dow.com.
88. Norris, A.W., M. Bahadur, and M. Yoshitake. *Novel silicone materials for LED packaging*. in *Fifth International Conference on Solid State Lighting*. 2005. International Society for Optics and Photonics.
89. Vanlathem, E., et al. *Novel silicone materials for LED packaging and optoelectronics devices*. in *Organic Optoelectronics and Photonics II*. 2006. International Society for Optics and Photonics.
90. Bahadur, M., et al. *Silicone materials for LED packaging*. in *Sixth International Conference on Solid State Lighting*. 2006. International Society for Optics and Photonics.
91. ClorDiSys, *Ultraviolet Light Disinfection Data Sheet*. 2020.
92. Jobling., R.K.H.a.M.G., *Chapter 5 Genetics*, in *Medical Microbiology. 4th edition*. 1996: Galveston (TX): University of Texas Medical Branch at Galveston.
93. Yamaguchi, U., M. Ogawa, and H. Takei, *Patterned Superhydrophobic SERS Substrates for Sample Pre-Concentration and Demonstration of Its Utility through Monitoring of Inhibitory Effects of Paraoxon and Carbaryl on AChE*. *Molecules*, 2020. **25**: p. 2223.

94. Canada, H., *ARCHIVED Guidance document - Safety and efficacy requirements for hard surface disinfectant drugs*, H. Canada, Editor. 2014, Government of Canada:
www.canada.ca.